International Journal of Applied Pharmaceutics

ISSN- 0975-7058 Vol 18, Issue 2, 2026

Original Article

DEVELOPMENT OF ANTI-INFLAMMATORY OIL MICROSPHERE AND EVALUATING THE ACTIVITY *IN VITRO AND IN VIVO*

VIJAYALAKSHMI P.[1,2], MALARKODI VELRAJ[1*]

[1]Department of Pharmacognosy, School of Pharmaceutical Sciences, Vels Institute of Science, Technology and Advanced Studies, Chennai, Tamil Nadu-600117, India. [2]Department of Pharmaceutical Technology, School of Health and Medical Sciences, Adamas University, Barasat, Kolkata, West Bengal-700126, India

*Corresponding author: Malarkodi Velraj; *Email: malarkodiv.sps@vistas.ac.in

Received: 26 May 2025, Revised and Accepted: 02 Feb 2026

ABSTRACT

Objective: *Citrus maxima* (Burm). Merr. (*C. maxima*) peel oil is traditionally used to relieve stress. Its antimicrobial, cardioprotective, hepatoprotective, and anti-inflammatory properties make it a versatile remedy. *C. maxima* hold immense potential in modern therapeutic applications. This study aimed to formulate and evaluate *Citrus maxima* microspheres for *in vitro* and *in vivo* anti inflammatory activity.

Methods: The present study was carried out using *Citrus maxima* peel oil extracted and GC-MS (Gas Chromatography-Mass Spectroscopy) was performed for complete chemical profiling. Microspheres were prepared using chitosan polymer with an emulsion chemical crosslinking approach and evaluated using SEM (Scanning Electron Microscopy), infrared spectroscopy, thermogravimetric assay, XRD (X-ray Diffraction), etc. *An in vitro* assay was performed using the inhibition of albumin denaturation assay and the membrane stabilisation method. *In vivo* anti-inflammatory activity as assessed using Carrageenan-Induced paw edema.

Results: GC-MS of *Citrus maxima* peel oil identified limonene (69.98%), beta-myrcene (6.23%), auraptene, alpha-pinene, and linalool as significant constituents. Formulation 1 (F1) showed the highest yield (79.28%), drug loading (84.28%), and encapsulation efficiency (78.32%) and also the highest swelling index (900.2%). The *in vitro* release of up to 72.03% in 8 h from F1 followed Higuchi kinetics (R^2 = 0.9859), suggesting diffusion-controlled release. Anti-inflammatory bioassays showed significant inhibition of protein denaturation and membrane lysis comparable to Diclofenac. *In vivo*, F1 microspheres at 400 mg/kg suppressed paw edema by 88.24%, approaching the activity of indomethacin (94.12%), establishing enhanced and sustained anti-inflammatory activity.

Conclusion: *Citrus maxima* oil-loaded microspheres exhibited enhanced anti-inflammatory activity in both *in vitro* and *in vivo* models. These findings suggest promising implications for the development of plant-based, biopolymer-encapsulated formulations as effective natural anti-inflammatory therapeutics.

Keywords: *Citrus maxima*, Chitosan microspheres, Anti-inflammatory activity, GC-MS, Carrageenan-induced paw edema

DOI: https://dx.doi.org/10.22159/ijap.2026v18i2.55226 Journal homepage: https://innovareacademics.in/journals/index.php/ijap

INTRODUCTION

In the context of modern pharmaceutical technology, microencapsulation is a beneficial method for modifying the physicochemical and biopharmaceutical characteristics of certain active ingredients [1]. In order to do this, biocompatible polymers that can trap bioactives have been utilized to improve its miscibility in aqueous food items, conceal off flavours, enhance site-specific targeted administration, and boost the stability of entrapped chemicals in food, cosmetic, cosmeceutical, and pharmaceutical industries [2]. In creating novel nano-and microformulations of natural bioactives, respectively, there is an increasing interest in using safe polymeric nano-and microdevices [3-5].

Pomelo, also known as *Citrus maxima*, is the largest citrus fruit in the Rutaceae family and native to South and Southeast Asia. It is rich in vitamin C, saponins, alkaloids, phenols, glycosides, terpenoids, amino acids, flavonoids, carbohydrates and carotenoids. The essential oils from the leaves and fruit peel contain nerolyl acetate, limonin, geraniol, and nerolol. (Xu G). Ethnopharmacological studies have shown that *C. maxima* has various pharmacological activities, including hepatoprotective, analgesic, antitumour, anti-inflammatory, hypocholesterolemic, antioxidant, and antidiabetic properties [6].

Chitosan is a biopolymer of β1→4 linked 2-amino-2-deoxy-glucopyranose and 2-acetamido-2-deoxy-β-D-glucopyranose residues that is produced by N-deacetylating chitin, a plentiful biopolymer isolated from the exoskeletons of crustaceans such as crabs and shrimps [7-11]. Due to its biocompatibility and mucoadhesion properties, chitosan has been used extensively for the microencapsulation of bioactive compounds. These applications include pulmonary, intestinal, and transdermal drug delivery, as well as being a useful compound for coating preformed magnetic nanotubes. Additionally, because of its positive charge, chitosan can interact with negatively charged substrates, like genetic components, promoting their complexation, intracellular transport, and protection [9].

The properties of chitosan can be utilized to enhance the pharmacological activity of pomelo oil, creating a microformulation with sustained action. Pomelo oil-loaded chitosan microspheres were prepared and evaluated using an emulsion chemical crosslinking approach. Pomelo oil is used worldwide and its pharmacological properties have been studied; however, no study has examined its anti-inflammatory properties. In this study, we used *in vitro* and *in vivo* models of inflammatory illnesses with pomelo oil extract and pomelo oil microspheres to establish its ethnomedicinal advantages against a variety of inflammatory diseases. The Particle size, encapsulation effectiveness, *in vitro* release behaviour, and *in vitro* release kinetics of the microspheres were assessed.

MATERIALS AND METHODS

Chemicals and drugs

Merck Life Science Pvt. Ltd. (Mumbai, India), and HiMedia Laboratories Pvt. Ltd. (Mumbai, India) provided chitosan, sodium hydroxide (NaOH), glacial acetic acid, methanol (analytical grade), hydrochloric acid (0.1 M), Bovine Serum Albumin (BSA), phosphate-buffered saline (PBS), normal saline, and n-alkanes (used for LRI calibration).

Carrageenan λ and Diclofenac sodium (Declophen®) were procured from Pharco Pharmaceuticals, available through wholesalers in

India. ELISA kits for TNF-α and IL-1β were acquired from ABclonal Technology and distributed in India by Biokart India Pvt. Ltd. and Genxbio Health Sciences Pvt. Ltd.

Perkin Elmer sells zinc selenide (ZnSe) ATR crystals for FTIR, Shimadzu sells alumina crucibles for TGA, and JEOL sells gold sputtering supplies for SEM.

Extraction of pomelo oil

Fresh pomelo (*Citrus maxima* Linn) fruits were collected from Jharkhand (latitudes 23.9586612°N and longitudes 86.8057714°E) of India in October 2023, authenticated by K. Karthigeyan, Scientist E, Central National Herbarium, Botanical Survey of India, Howrah, with an authentication no CNH/Tech. II/2023/21. The ripe fruits were thoroughly rinsed and fruit peels were separated and air dried for 8-10 d. The peels (200 g) were transferred into a round-bottom flask and extracted using a Clevenger apparatus for 8 h. The Oil extracted was collected and stored in an amber colored glass vial, sealed, and kept at 4 °C for further use.

Yield of pomelo peels oil (Y) obtained for every run was calculated as follow [12]:

$$Y\ (\%) = \frac{\text{Volume of essential oil(ml)}}{\text{Amount of raw materials (g)}} \text{ X } 100$$

GC-MS sample preparation and analysis of pomelo oil

To prepare the sample for GC-MS, 5 ml of the extracted oil was dissolved in methanol. After centrifuging the solution at 3000 rpm for 15 min, an aliquot of 1 µl** was injected for GC -MS analysis. The content of the volatile oil is expressed as a percentage of v/w. A Shimadzu gas chromatograph with a SE-30 10% Chromos orb-W packed stainless steel column (2 m x 2 mm) was used to perform GC-MS. Oven programme: 60 °C (5 min), 60°-260 °C (5 °C/min), 260 °C (10 min); carrier gas – nitrogen, flow rate 40 ml/min; injector temperature 240 °C; detector temperature 240 °C. Individual components were identified by matching the mass spectra with available literature in different libraries, such as WILEY and NIST by comparing their mass spectrum values. The Linear Retention Index (LRI) of a compound is an expression of its retention time on a gas chromatographic column relative to the homologous series n-alkanes. The below mentioned equation is used to calculate the LRI from the retention time [13].

$$\text{LRI} = 100\ (\frac{t-tn}{tn-1-tn} + n)$$

t = retention time of component

n = carbon number of preceding n-alkane

n+1 = carbon number of subsequent n-alkane

Preparation of microspheres

A 2% chitosan solution (w/v) was prepared using a 1% aqueous acetic acid solution and stirred using a mechanical stirrer at 1,500 revolutions per minute (rpm) for 2 h. Pomelo oil was added and stirred continuously for 2 h. Microspheres were prepared using an emulsion-droplet coalescence method. The essential oil-containing emulsion was then dripped into 100 ml solutions that included 1% NaOH solution with slight modification as developed ealier [14]. The obtained microspheres were washed, filtered, and dried at 30 °C for 24 h. Three batches were prepared as per the factorial design [15, 16]. The amount of drug (Pomelo oil) concentration was varied in batches F1, F2 and F3 as shown in table 1 below.

Table 1: Formulation of pomelo oil microsphere

Formulation	Formulation 1 (F1)	Formulation 2 (F2)	Formulation 3 (F3)
Pomelo oil (ml)	5	10	15
2% Chitosan solution (ml)	95	90	85

Evaluation of the microspheres

Percentage yield, encapsulation efficiency, and drug loading

The Percentage yield (%Y) was evaluated based on the weight of the microsphere, polymer, and drug used in the preparation of the emulsions and the final weight after drying, using the following equation:

$$\%\ \text{Yield} = \frac{\text{Actual weight}}{\text{Theoreitical weight}} \text{ X } 100$$

Drug loading and encapsulation efficiency

The drug loading (DL) and encapsulation efficiency (EE) of the prepared formulation were assessed using established methods with slight modifications [17]. An accurately weighed amount of drug-loaded particles was dissolved in an appropriate solvent to release the drug. The solution was ultrasonicated for 15 min to facilitate complete dissolution. The mixture was centrifuged at 10,000 rpm for 10 min to separate undissolved excipients or particles. The clear supernatant was collected and analysed using a UV-Visible spectrophotometer at the characteristic wavelength of the drug (e. g., 265 nm for drug X). The drug concentration in the supernatant was quantified using a pre-determined calibration curve [18].

The following equations were employed to calculate the percentage drug loading and encapsulation efficiency:

1. Percentage drug loading (DL): $\frac{Actual\ drug\ content}{Weight\ of\ microsphere} X\ 100$

2. Percentage encapsulation efficiency (EE): $\frac{\text{Actual drug content}}{\text{Theoritical drug content}} \text{ X } 100$

The experiments were conducted in triplicate, and the results are expressed as the mean±Standard Error of the mean (SEM). For validation of the analytical method, linearity, accuracy, and precision were assessed as per ICH guidelines

Particle size analysis

A compound microscope was used to perform particle size analysis of the drug-loaded chitosan microspheres. A small quantity of dry microspheres was suspended in purified water (10 ml) and ultrasonicated for 5s. A small drop of the obtained suspension was placed on a clean glass slide. The slide containing chitosan microspheres was mounted on the stage of the microscope and diameter of minimum 300 particles was measured using a calibrated ocular micrometer [13].

Swelling index

The microspheres (10 mg) were immersed for 24 h at 37 °C in 100 ml of 0.1M HCl. After a day, the microspheres were pulled out, and the remaining HCl was removed with filter paper. The ultimate weight of microsphere was then determined. By using the following formula, the swelling index of the various microsphere formulations was calculated [19].

$$\text{Swelling index} = \frac{Wt-Wo}{Wo} \text{ X } 100$$

Where W_t = weight of microspheres observed at 24 h

Wo = initial weight of microspheres

Infrared spectroscopy (FT-IR)

Infrared spectra were collected at a scan range of 500–4000 cm^{-1}using a Frontier FTIR/NIR spectrophotometer (Perkin Elmer, USA, Frontier) with an attenuated total reflectance (ATR) accessory with zinc selenite crystal (ZnSe) at a resolution of 4 cm^{-1} and an arithmetic mean of eight scans [20].

Thermogravimetry

Thermogravimetric (TG) curves were obtained using a TGA/SDTA 851e thermal analyzer (Shimadzu Corporation, Japan; DTG-60) under an inert atmosphere, and the following analytical conditions: a flow rate 50 ml/min, heating rate of 10 °C/min and temperature range between 30 and 600 °C, using alumina (aluminium oxide) crucible containing approximately 5 mg of sample. The parameter used to determine the initial degradation temperature was T_{onset}, obtained by the intersection of a tangent drawn between the upper and lower horizontal base lines and the steep part of the sigmoidal curve, characterizing the point that best represents the degradation temperature of a compound [21].

X-ray powder diffractometry (X-RD)

The effect of the microencapsulation process on drug-crystallinity was investigated using X-ray powder diffractometry, as described previously [10]. Powder X-RD patterns were recorded on Rigaku (Model-Rigaku, Japan; Smart Lab 9KW) using Ni-filtered, Cuk α radiation, a voltage of 30 kV and a current of 25 mA. The scanning rate employed was 2 /min, over 4° to 40° diffraction angle (2θ) range. The X-RD patterns of drug-loaded microspheres and drug powder were recorded in comparison to the empty chitosan [22].

Morphology of microspheres

The surface morphologies of the microspheres were analyzed using a JEOL JSM 6360 Scanning Electron Microscope (SEM). Samples were mounted on conductive adhesive tape, sputter-coated with gold, and imaged at 10 kV accelerating voltage under secondary electron mode. The method follows standard SEM imaging protocols as described by Goldstein *et al.* [23].

Drug entrapment

The drug entrapment efficiency of microspheres was determined using UV-Vis spectrophotometry. The microspheres were dissolved in 0.1 M HCl under constant stirring, and the solution was filtered to remove undissolved particles. The absorbance of the filtrate was measured at the characteristic wavelength of 217 nm, and the entrapment efficiency was calculated using the formula described by Venkatesan *et al.* in (2009). The drug content of each sample was determined in triplicate, and the results were averaged [24].

***In vitro* drug release studies**

Solubility studies for sink condition validation

The solubility of Citrus maxima peel oil in the dissolution medium (0.1N HCl containing 0.5% w/v Tween 80) was determined using the shake flask method to ensure sink conditions for the *in vitro* drug release study. An excess amount of C. maxima oil was added to 10 ml of the dissolution medium in a capped conical flask. The mixture was agitated in a water bath shaker at 100 rpm and 37±0.5 °C for 24 h to attain equilibrium. The samples were then filtered through whatman no. 1 filter paper and appropriately diluted with methanol. The concentration of the dissolved oil was determined by UV-Vis spectrophotometry at 217 nm. Each experiment was carried out in triplicate, and the mean solubility (mg/ml) was calculated.

The release of Citrus maxima peel oil from chitosan microspheres for oral anti-inflammatory activity was evaluated, and an *in vitro* release experiment of the drug was conducted using a USP dissolution testing apparatus II (basket type) with a rotation rate of 50 rpm and a temperature of 37±0.5 °C. To enhance the solubility of the hydrophobic oil and provide sink conditions, a dissolution medium composed of 900 ml of 0.1N HCl containing 0.5% w/v of Tween 80 was employed.

Microspheres loaded with pomelo oil content were put in the basket and then placed to the medium. Every hour for 8 h, 5 ml samples were removed and immediately replaced with fresh pre-warmed medium. The samples were filtered through Whatman No. 1 filter paper, and the absorbance of each sample was determined at 217 nm by a UV-Visible spectrophotometer. The cumulative percentage release of the drug was determined from the calibration curve of the absorbance values run in the same medium [25-27].

***In vitro* release kinetics**

The cumulative release percentage was calculated and plotted against the time. Dissolution data from the above methods was fitted to Zero order, First order and Higuchi equations. The mechanism of drug release was determined by using Korsmayer Peppas equation [28, 29].

***In vitro* anti-inflammatory activity**

Inhibition of albumin denaturation assay

The anti-inflammatory activity was determined by measuring the inhibition of heat-induced denaturation of Bovine Serum Albumin (BSA). A reaction mixture of 1% (w/v) BSA in PBS (pH 6.4) with different concentrations of the test sample was incubated at 37 °C for 15 min followed by heating at 70 °C for 5 min. After cooling, the absorbance was measured at 660 nm wavelength. Diclofenac sodium was used as a reference, and the percentage inhibition was obtained as per the method described by Sakat SS, Juvekar AR, and Gambhire MN [30, 31].

Membrane stabilisation method

The anti-inflammatory activity was assessed by evaluating the membrane-stabilizing effect on Red Blood Cell (RBC) membranes. Blood was drawn from human participants and diluted with isotonic saline. The test sample (0.1–1 mg/ml) was added to 1 ml of RBC suspension and incubated at 37 °C for 30 min, followed by centrifugation. The absorbance of the supernatant at 560 nm was determined. The percentage inhibition of hemolysis was determined by comparing the test sample with the control group. Diclofenac sodium was employed as the reference standard, as reported earlier [30].

***In vivo* tests**

Wistar rats weighing 350-375 g were employed in this study. The animals were obtained from the Establishment of Environment Controlled Facilities at CLART to be housed at the Rabbit Shed of the Centre for Laboratory Animal Research and Training (CLART) at Kalyani, Nadia, West Bengal-741,235 during the 2024-2025 term. The animals were housed in Adamas University's School of Health and Medical Sciences (2163/PO/Re/S/22), West Bengal, India. Each animal was provided with a sufficient supply of food and water. The room temperature was 20±2 °C, with a 12 h light/dark cycle starting at 8:00 a. m. Before beginning any pharmacological testing, a minimum 24 h acclimatization period was provided. All animal tests were approved by The Adamas University's Institutional Animal Ethics Committee (IAEC), Department of Pharmaceutical Technology (Approval No. Au/SoHMS/DoPT/2024/CCSEA/P-13).

Acute toxicity

The wistar rats weighing 350-375 g were housed at the Rabbits Shed for 48 h to help them acclimatize before being subjected to the study. The animals were fasted (3-4 h) by withholding food but not water. The animals were given a single dose of extract at a dose of 2000 mg/kg. As medicinal plants are generally considered safe, at their highest dose level (2000 mg/kg) as per OECD guideline 423.

The animals were monitored for, appearance of mucous membrane, skin fur, eyes, coma, lethargy, sleep, convulsions, salivation, tremors, diarrhoea, body weight deviation, and mortality and recorded after 0.5 hour, 1 hour, 4 h, 24 h, 48 h, 7 d, and 14 d respectively [32, 33].

***In vivo* anti-inflammatory activity**

Caregeenan-induced paw edema

The oral doses of 200 and 400 mg/kg of *Citrus maxima* peel oil and its microsphere formulations were selected based on prior reports using similar doses for anti-inflammatory activity in *Citrus* species [34]. These doses also showed no toxicity in our acute oral study up to 2000 mg/kg, confirming their safety and relevance for pharmacological evaluation. By inducing paw edema with carrageenan, the protective impact of several *Citrus maxima oil*-loaded microsphere formulations was examined. The following formulas were used to inoculate the rats, which were split up into six

groups of six animals each: i) saline, ii) indomethacin (10 mg/kg), iii) *Citrus maxima* oil 200 mg/kg, iv) *Citrus maxima* oil 400 mg/kg, v) *Citrus maxima* oil Microsphere oil 200 mg/kg and vi) *Citrus maxima* oil Microsphere oil 400 mg/kg after one hour, 0.1 ml (1% w/v) of carrageenan was injected into the plantar surfaces of the rats' hind paws to induce acute inflammation using the method adopted earlier with slight modification [35]. A mercury plethysmograph was used to measure the paw volume following the carrageenan injection. One helpful metric for forecasting the protective effectiveness of the various formulations was the difference between the volume of the carrageenan-injected paw and the control paw. The progression of paw edema was measured at 0, 1, 2, 3, 4, and 5 hour intervals using Vernier digital calliper [36, 37].

Compared to the control groups, which received the vehicle, the percentage of edema inhibition was calculated using the formula:

$$\text{Inhibition\%} = \frac{\text{Change in Control} - \text{Change in treatment}}{\text{Change in control}} \text{ x } 100$$

Table 2: Constituents present in *Citrus maxima* oil with their RT time, chemical formula, molecular weight, composition (area %) and chemical class by GC-MS

No. of peak	Rt (min)	Chemical constituents	Formulas	Composition (Area %)	Molecular weight	Chemical class
1	1.165	Silane, dimethyl-	C_2H_8Si	1.88	60	Metalloid Compounds
2	4.544	. alpha.-Pinene	$C_{10}H_{16}$	2.04	136	Aromatic Terpenes
3	5.152	Bicyclo[3.1.0]hexane, 4-methylene-1-(1-methylethyl)	$C_{10}H_{16}$	1.84	136	Bicyclic Monoterpenes
4	5.434	beta-Myrcene	$C_{10}H_{16}$	6.23	136	Aliphatic unsaturated
5	5.678	Octanal	$C_8H_{16}O$	1.37	128	Caprylic aldehyde
6	6.306	Bicyclo[4.1.0]heptane, 7-(1-methylethylidene)-(Limonene)	$C_{10}H_{16}$	69.98	136	Bicyclo terpenes
7	6.385	1,3,6-Octatriene, 3,7-dimethyl-, (E)-	$C_{10}H_{16}$	0.19	136	Acyclic Monoterpenes
8	6.524	1,4-Cyclohe..adiene, 1-methyl-4-(1-methylethyl)-	$C_{10}H_{16}$	0.12	136	Cyclohe..ane monoterpenes
9	6.696	Cyclopropane, pentyl-	C_8H_{16}	0.11	112	Cyclo aliphatic alkane
10	6.730	. alpha.-Methyl-. alpha.-[4-methyl-3-pentenyl]oriranemethanol	$C_{10}H_{18}O_2$	0.08	170	Aliphatic alcohol
11	7.116	1,6-Octadien-3-ol, 3,7-dimethyl-	$C_{10}H_{18}O$	0.56	154	Acyclic Monoterpenes
12	7.426	trans-p-Mentha-2,8-dienol	$C_{10}H_{16}O$	0.21	152	Aromatic terpenes
13	7.614	7-Oxabicyclo[4.1.0]heptane, 1-methyl-4-(1-methylethenyl)-	$C_{10}H_{16}O$	0.85	152	Cyclohexane Monoterpenes
14	7.681	Limonene oxide, trans-	$C_{10}H_{16}O$	0.39	152	Cyclohexane monoterpenes
15	7.901	6-Octenal, 3,7-dimethyl-, (R)-	$C_{10}H_{18}O$	0.12	154	Acyclic Monoterpenes (aldehyde of citronellol)
16	8.261	2-Isopropenyl-5-methylhex-4-enal	$C_{10}H_{16}O$	0.07	152	Unsaturated aliphatic terpene
17	8.466	3-Cyclohexene-1-methanol,. alpha.,. alpha.4-trimethyl-	$C_{10}H_{18}O$	0.22	154	Cyclohexane Monoterpenes
18	8.536	p-Mentha-1,8-dien-9-ol	$C_{10}H_{16}O$	0.10	152	Aromatic
19	8.584	1,3,6-Heptatriene, 2,5,6-trimethyl-	$C_{10}H_{16}O$	0.08	152	Aliphatic Terpene
20	8.665	Decanal	$C_{10}H_{20}O$	1.54	156	Aliphatic aldehyde
21	8.748	Acetic acid, octyl ester	$C_{10}H_{20}O_2$	0.22	172	Aliphatic acetate
22	8.885	2-Cyclohexen-1-ol, 2-methyl-5-(1-methylethenyl)-, trans-	$C_{10}H_{16}O$	0.26	152	limonene monoterpenoid
23	9.055	2-Cyclohexen-1-ol, 2-methyl-5-(1-methylethenyl)-, cis-	$C_{10}H_{16}O$	0.17	152	limonene monoterpenoid
24	9.186	2,6-Octadienal, 3,7-dimethyl-, (Z)-	$C_{10}H_{16}O$	0.09	152	Acyclic Monoterpenes
25	9.233	2-Cyclohexen-1-one, 2-methyl-5-(1-methylethenyl)-(Carvone)	$C_{10}H_{14}O$	0.32	150	Cyclohexane Monoterpenes
26	9.603	2,6-Octadienal, 3,7-dimethyl-, (E)-(Citral)	$C_{10}H_{16}O$	0.18	152	Acyclic Monoterpenes
27	10.111	2-Cyclohexen-1-ol, 1-methyl-4-(1-methylethenyl)-, trans-	$C_{10}H_{16}O$	0.18	152	p-menthane monoterpenoid
28	10.860	Bicyclo[2.2.1]heptane-2,5-diol, 1,7,7-trimethyl-, (2-endo,5-exo)-	$C_{10}H_{18}O_2$	0.15	152	Terpenoids
29	11.017	Copaene	$C_{15}H_2$·	0.23	170	Sesquiterpenes
30	11.104	2,6-Octadien-1-ol, 3,7-dimethyl-, acetate, (E)-	$C_{12}H_{24}O_2$	0.38	204	Acetates
31	11.205	1H-Cyclopenta[1,3]cyclopropa[1,2]ben..ene, octahydro-7-methyl 3 methylene-4-(1-methylethyl)	$C_{15}H_{24}$	0.48	200	Tricyclic sesquiterpene
32	11.442	Acetic acid, decyl ester	$C_{12}H_{24}O_2$	0.27	204	Car..oxylic ester
33	11.606	Caryophyllene	$C_{15}H_{24}$	0.20	200	Polycyclic Sesquiterpenes
34	12.029	. alpha.-Caryophyllene	$C_{15}H_{24}$	1.53	204	Monocyclic Sesquiterpenes
35	12.397	Germacrene D	$C_{15}H_{24}$	0.20	204	Sesquiterpenes
36	13.004	Naphthalene, 1,2,3,5,6,8a-hexahydro-4,7-dimethyl-1-(1-methylethyl)-, (1S-cis)-	$C_{15}H_{24}$	0.10	204	sesquiterpene
37	13.447	3,7· Cyclodecadiene-1-methanol,. alpha.,. alpha.,4,8-tetramethyl	$C_{15}H_{26}O$	0.29	204	Sesquiterpene
38	13.976	Spathulenol	$C_{15}H_{24}O$	0.05	222	Sesquiterpenes
39	14.082	Caryophyllene oxide	$C_{15}H_{24}O$	0.06	220	Polycyclic Sesquiterpenes
40	17.493	2(3H)-Naphthalenone, 4,4a,5,6,7,8-hexahydro-4,4a-dimethyl-6-(1 methylethenyl)-	$C_{15}H_{22}O$	0.32	220	Sesquiterpenoid
41	19.328	Eicosanoic acid	$C_{20}H_{40}O_2$	0.31	218	Fatty Acids
42	21.079	11,14-Eicosadienoic acid, methyl ester	$C_{21}H_{38}O_2$	0.14	312	Aliphatic Fatty Acids
43	21.129	Erucic acid	$C_{22}H_{42}O_2$	0.10	322	Fatty Acids, Monounsaturated
44	21.170	Osthole	$C_{15}H_{16}O_3$	0.09	338	Coumarins (Benzopyrans)
45	22.116	2H-1-Benzopyran-2-one, 7-methoxy-6-(3-methyl-2-oxobutyl)-	$C_{15}H_{16}O_4$	0.17	244	Aromatic
46	22.162	2H-1-Benzopyran-2-one, 4-methyl-3-propyl-	$C_{13}H_{14}O_2$	0.36	260	Aromatic
47	22.523	2-Furancarboxaldehyde, 5-[(5-methyl-2-furanyl)methyl]-	$C_{11}H_{10}O_3$	0.31	202	Aromatic aldehyde
48	23.399	Pentacosane	$C_{25}H_{52}$	0.26	190	Hydrocarbons, Acyclic
49	25.282	2H-1-Benzopyran-2-one, 7-[(3,7-dimethyl 2,6-octadienyl)oxy]-, (E)-	$C_{19}H_{22}O_3$	0.03	352	Coumarins
50	26.237	2,2-Dimethyl-3-[3-methyl-5-(phenylthio)pent-3-enyl]oxirane	$C_{16}H_{22}OS$	0.07	262	Aromatic
51	26.494	Oxirane, 3-[5-(4-azidophenoxy)-3-methyl-3-pentenyl]-2,2-dimethyl-, (E)-..·/-.-	C_1 $H_{21}N_3O_2$	0.17	287	Aromatic
52	26.688	2,6,10,14,18-Pentamethyl-2,6,10,14,18-eicosapentaene	$C_{25}H_{42}$	0.05	342	Aliphatic terpene
53	26.729	Tetracosanal	$C_{24}H_{48}O$	0.08	352	fatty aldehyde
54	27.141	1-Ethyladamantan-2-ol	$C_{12}H_{20}O$	0.03	352	Aliphatic Cyclic Hydrocarbons
55	28.458	Z-2-Octadecen-1-ol	$C_{18}H_{36}O$	0.05	352	Aliphatic alcohol
56	29.114	4',5,6,7,8-Pentamethoxyflavone	$C_{20}H_{20}O_7$	0.06	372	Flavones
57	30.059	Gamma.-Sitosterol	$C_{29}H_{50}O$	0.14	414	Sitosterols
58	30.361	Androst-4-ene-3,17-dione, 12-[(trimethylsilyl)oxy]-, bis(O-methyloxime), (12. beta.)-	$C_{24}H_{40}N_2O_3Si$	0.11	432	Steroid
59	31.980	Friedelin	$C_{30}H_{50}O$	0.11	426	Pentacyclic Triterpenes
60	32.824	Pentacyclo[19.3.1.1(3,7).1(9,13).1(15,19)]octacosa-1,3,5,7,9,11,13,15,17,19	$C_{44}H_{56}O_4$	0.06	648	Aromatic arenes

Statistical analysis

All experiments were performed in triplicate, and the results were shown as the mean±Standard Error of the Mean. GraphPad Prism 8.0.2 software (Boston, MA, USA) was used for statistical calculation. The significance difference and difference at P-value<0.05 were determined using Tukey's multiple comparison test.

RESULTS AND DISCUSSION

Essential oil extraction

The oil was extracted from the dried peel of pomelo fruit using Clevenger's apparatus. The oil was pale yellow, highly aromatic and the yield of the oil was calculated as 3%.

GC-MS sample preparation and analysis of pomelo oil

The chemical profile of pomelo oil fraction was analysed by GC–MS, which showed the presence of following compounds. Description of all the constituents present along with their RT time, chemical formula, Molecular weight, Composition (area %) and chemical class is given in table 2.

Analyses of GC–MS data exhibited four major chemical classes, namely, Terpenes (52%), aromatic alkanes and arenes (11%), aldehyde (8%) and Fatty acids and esters (7%). Rest of the compounds constituting acetates coumarins, flavones, steroids and sitosterol's, alcohol and alkanes are 3% each and rest constituents were placed as miscellaneous group which was about 5%.

The main constituents of *Citrus maxima* peel oil were found to be DL-limonene (69.98%), Beta-Myrcene (6.23%), 2H-1-Benzopyran-2-one, 7-[(3,7-dimethyl-2,6-octadienyl) oxy] (2.78%), Silane, dimethyl (1.88%), Bicyclo [3.1.0] hexane, 4-methylene-1-(1-methylethyl) (1.84%), Decanal (1.54%), Octanal (1.37%), 7-Oxabicyclo [4.1.0] heptane, 1-methyl-4-(1-methylethenyl) (0.85%), and Linalool (0.56%).

Citrus maxima peel essential oil has strong anti-inflammatory qualities and is high in DL-limonene (69.98%) and β-myrcene (6.23%). One important monoterpene, DL-limonene, has been shown to reduce inflammation and oxidative stress by blocking pro-inflammatory cytokines like TNF-α and IL-6[38]. Like non-steroidal anti-inflammatory medications, β-Myrcene also has anti-inflammatory properties by reducing leukocyte migration and altering COX-2 expression [39]. It has been demonstrated that minor components like linalool (0.56%) inhibit NF-κB activation, thereby reducing inflammatory reactions [40]. Furthermore, because of their capacity to regulate oxidative pathways and lipid peroxidation, decanal (1.54%) and octanal (1.37%) have been linked to anti-inflammatory effects [41]. According to these findings, *Citrus maxima* peel oil may have therapeutic uses in treating inflammatory diseases.

Percentage yield, encapsulation efficiency, and drug load

The yield percentage of *Citrus maxima* oil-loaded microspheres varied with the formulation composition. The highest yield was observed in formulation F1 (79.28±0.42%), followed by F2 (73.66±0.35%), and the lowest in F3 (69.05±0.67%). The yield reduction from F1 to F3 may be due to the rising polymer concentration or differences in crosslinking efficiency that could have led to higher material loss during washing or drying processes. This is in line with earlier research where increased viscosity and dense crosslinking prevented microsphere recovery [42, 43].

Drug loading efficiency also showed a strong reduction throughout the formulations, and F1 presented the highest result (84.28±0.36%), followed by F2 (73.66±0.22%) and F3 (68.05±0.22%). This reflects that the decreased polymer content in F1 entrapment accommodated more *Citrus maxima* oil inside the microspheres. With the increase in polymer concentration F2 and F3, the encapsulation matrix may have become denser, thus minimizing the diffusion and resulting into entrapment of the oil into the core. Similar results have been described in encapsulation studies of essential oils, in which matrix density was inversely correlated with drug loading [44, 45].

The (EE) followed the same trend as drug loading, where F1 had the highest EE (78.32±0.26%), followed by F2 (68.44±0.18%) and F3 (66.82±0.24%). The reduction in EE in F2 and F3 is possibly due to the mismatch in the ratio of polymer to oil, which possibly resulted in leakage of the oil partially during the emulsification and crosslinking processes. Nguyen *et al.* (2024) emphasized the need to tailor oil-to-polymer ratios for maximum EE in alginate-chitosan encapsulation systems.

The observed decline in encapsulation efficiency and yield at higher oil concentrations (F3) may be due to the saturation of the chitosan polymer matrix. At lower oil concentrations (F1), the oil is effectively encapsulated within the chitosan network, resulting in higher efficiency. However, as oil concentration increases (F3), the polymer may reach its maximum capacity to entrap the oil, leading to surface deposition or leakage of excess oil during the emulsification or curing stages. This phenomenon can also reduce microsphere yield due to loss of oil or structural instability. Furthermore, SEM images support this explanation by showing more porous and irregular structures in F3 compared to F1, indicating compromised encapsulation integrity at higher oil loads. Similar saturation and leakage effects have been reported in oil-loaded biopolymer systems [43, 44].

Particle size of the microspheres was raised from F1 (940.03 µm) to F2 (988.04 µm) and F3 (1046.67 µm). This is due to the increased polymer concentration in subsequent formulations, which most probably increased the viscosity of the dispersion medium, resulting in larger droplets during emulsification. A direct correlation between polymer concentration and microsphere size has been amply documented in the literature [46]. Larger particle sizes in F3 may also affect the release profile of the encapsulated oil, promoting a slower and more controlled release. All the encapsulation parameters of *Citrus maxima* oil-loaded microspheres are represented in table 3.

Table 3: Encapsulation parameters of *Citrus maxima* oil-loaded microspheres

Microsphere	F1	F2	F3
Yield %	79.28± 0.42	73.66±0.35	69.05±0.67
Drug loading %	84.28±0.36	73.66±0.22	68.05±0.22
Encapsulation efficiency %	78.32±0.26	68.44±0.18	66.82±0. 24
Particle size (µm)	940.03 µm	988.04 µm	1046.67µm

Data are means of three replicates (n = 3)±SEM

The results show that F1, having the lowest polymer content, yielded microspheres of higher yield, drug loading, and encapsulation efficiency, yet with a relatively smaller particle size. This implies that F1 is the most effective formulation for encapsulating Citrus maxima oil through the use of a chitosan polymer matrix.

Compared to the usual chitosan–alginate beads, which have a tendency towards burst release and have rapid swelling behaviors, the chitosan-alone microspheres studied here (specifically F1) had higher structural integrity and sustained drug release profile [47]. Studies with alginate–chitosan matrices have shown that encapsulation efficiencies are usually between 60% and 70% with significant burst effects in acidic conditions due to Ca^{2+} ion exchange. The opposite was true with F1 microspheres, having a higher encapsulation efficiency of 78.32% and lower initial burst, presumably due to more compact crosslinking and better oil

entrapment [48]. Such a feature renders the current formulation more suitable for bioactive oils like those obtained from *C. maxima*, which require controlled release mechanisms to realize maximum therapeutic efficacy.

Encapsulation of the volatile oils, such as *Citrus maxima* in chitosan microspheres presents potential uses in pharmaceuticals, cosmetology, and foodstuffs, where stability and controlled release are desired. In addition, the biocompatibility and biodegradation of chitosan render the system environmentally friendly and beneficial for therapeutic purposes.

Swelling index

The swelling index of *Citrus maxima* oil microspheres entrapped in chitosan were tested at pH 1.2, which mimics gastric conditions. The average swelling indices (in %±SEM) of the three formulations (F1–F3) are represented in fig. 1 below.

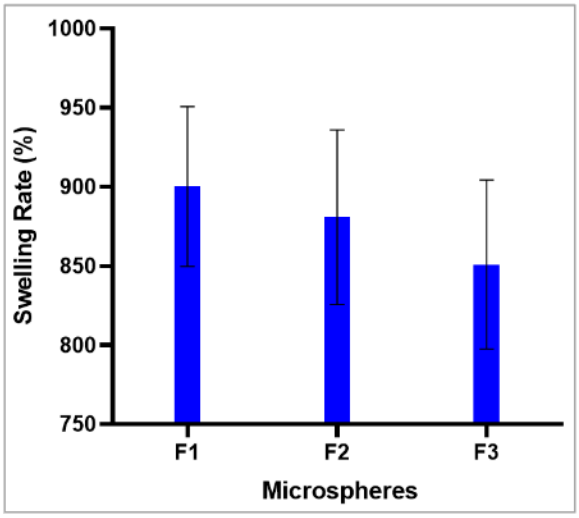

Fig. 1: % swelling rate of *Citrus maxima* oil microspheres at pH 1.2 (mean±SEM, n=3)

Swelling property in chitosan microspheres is a key determinant of their performance in gastro-retentive drug delivery systems. Chitosan is protonated at its amine groups under acidic conditions (pH 1.2), leading to higher electrostatic repulsion and water absorption [49]. The same was observed in the present study, wherein F1 recorded the maximum swelling index (900.2±50.5%), possibly due to the ideal chitosan concentration and crosslinking that favoured greater hydration and matrix expansion.

Formulation F2 closely trailed with a swelling index of 880.72±55.3%, whereas F3 showed dramatically reduced swelling (850.9±53.4%), perhaps as a result of a more compact matrix or enhanced hydrophobic oil content, both of which can restrict water intrusion and network relaxation [50]. These findings are in line with previous research that showed decreased swelling in formulations with increased oil-to-polymer ratios and denser crosslinking networks [51].

Swelling capacity also depends on drug release kinetics. Exaggerated swelling tends to increase more rapid diffusion of the trapped compound because of the more porous and water-swollen matrix [52]. Still, over-swelling can degrade mechanical stability, indicating the importance of a well-balanced strategy for formulation. Chen *et al.* has reported that moderate swelling is beneficial as it increases mucoadhesion and extends gastric residence time and makes such a system suitable for targeting the stomach [53]. Overall, the results support the hypothesis that controlled manipulation of chitosan concentration, crosslinking, and oil loading directly influences the swelling behaviour and, consequently, the drug release characteristics of *Citrus maxima* oil-loaded microspheres.

Drug excipient interaction study

Infrared spectroscopy

FTIR (Fourier Transform Infrared Spectroscopy) was employed to analyze the functional groups of pure *Citrus maxima* (pomelo) peel oil and the microsphere preparation. FTIR spectra serve to validate encapsulation by showing possible chemical interactions between the polymer (chitosan) and the oil.

FTIR spectrum of pomelo peel oil (fig. 2a)

3751.6 cm^{-1} and 3357.5 cm^{-1} – Broad bands showing O–H stretching vibrations, characteristic of alcohols and phenolic compounds found in essential oils [44].

2920.5 cm^{-1} – C–H asymmetric stretching of aliphatic –CH_2 groups, characteristic of long-chain hydrocarbons and terpenoids.

1632 cm^{-1}, 1597.3 cm^{-1} – Characteristic of C=C stretching in aromatic compounds and alkenes.

1373.5 cm^{-1} and 1154.2 cm^{-1} – C–H bending along with the C–O stretching vibrations, characteristic of esters or ethers.

794.1 cm^{-1} and 886 cm^{-1} – Aromatic or aliphatic C–H bond out-of-plane bending vibrations.

These peaks attest to the occurrence of important bioactive constituents such as limonene, α-pinene, and citral, widely documented in citrus essential oils [34].

FTIR spectrum of microsphere containing pomelo oil (fig. 2b)

2923.3 cm^{-1}, 2964.1 cm^{-1} – C–H stretching vibrations of remaining aliphatic chains of the oil within the microsphere.

1744.6 cm^{-1} and 1644.8 cm^{-1} – Carbonyl (C=O) and amide I regions, indicative of interaction with chitosan polymer [44].

1435.6 cm^{-1}, 1277.8 cm^{-1}, 1155.0 cm^{-1} – Indicative of C–N and C–O stretching in oil esters and chitosan.

1119.5 cm^{-1}, 856.6 cm^{-1} – Ether and aromatic ring bending vibrations, indicative of the fact that important functional groups of the oil are maintained after encapsulation.

The appearance of additional peaks in the range 528–406 cm^{-1} may suggest potential physicochemical interactions between Citrus maxima oil and the chitosan polymer. However, this interpretation is preliminary, as FTIR alone cannot conclusively confirm hydrogen bonding or specific interactions.

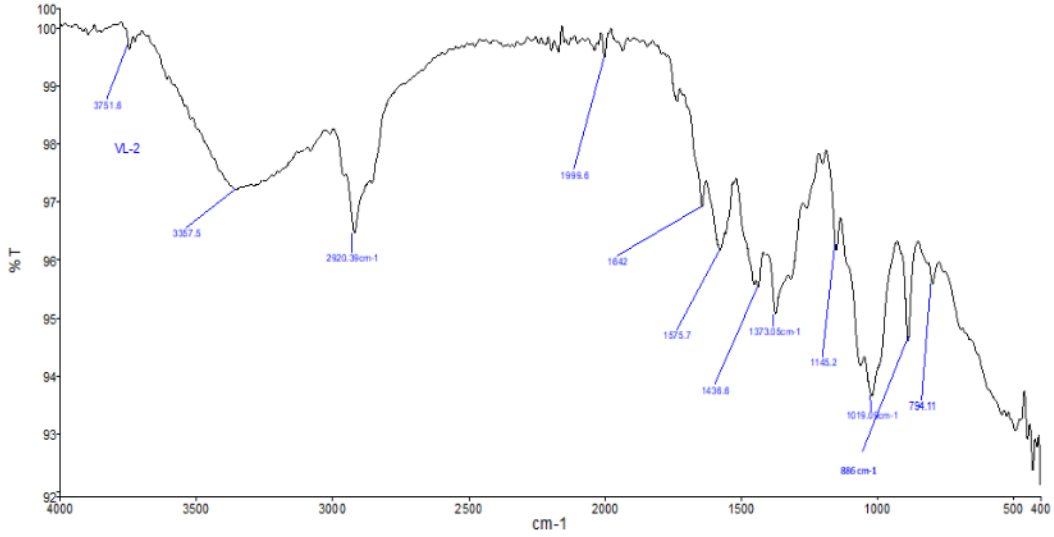

a)

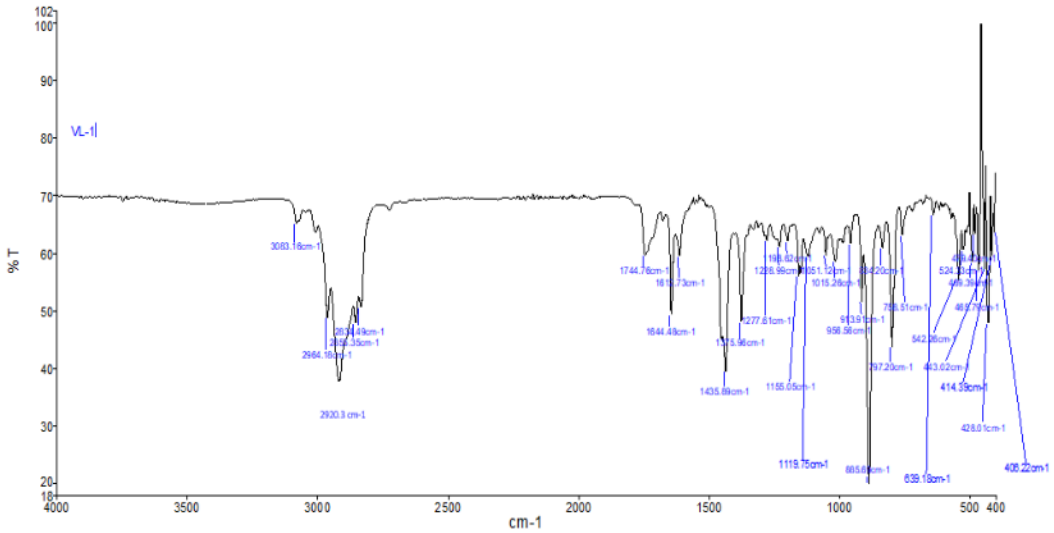

b)

Fig. 2: FTIR spectra of (a) Citrus maxima oil and (b) Citrus maxima oil-loaded chitosan microspheres. Prominent absorption peaks include O–H stretching (~3421 cm^{-1}), C–H stretching (~2923 cm^{-1}), C=O stretching (~1637 cm^{-1}). and C–N bending (~1380- 1020 cm^{-1}), confirming successful encapsulation without major structural alteration

The occurrence of characteristic peaks of chitosan and pomelo oil in the microsphere FTIR spectrum, and peak shifts or broadening, indicates successful encapsulation and possible molecular interactions. These are due to van der Waals' interactions or hydrogen bonding between the oil and chitosan [54].

This is reaffirmed by current research that shows that the encapsulation of essential oils in natural polymers results in functional group retention and better stability of volatile compounds [47]. The load of bioactive oils in polymeric carriers such as chitosan also increases sustained release, bioavailability, anti-inflammatory and antimicrobial activity [48]. FTIR studies prove that the principal functional groups of pomelo peel oil are maintained after encapsulation. The changes in the position of peaks and new peak formations in the spectrum of microspheres show evidence of interactions between the chitosan matrix and the oil, substantiating the efficacy of encapsulation. Results align with those found in the literature and highlight the applicability of chitosan-based microspheres in the regulated release of citrus essential oils.

TGA and DTA analysis

The thermal performance of *Citrus maxima* oil-loaded chitosan microspheres was evaluated using Thermogravimetric Analysis (TGA) and Differential Thermal Analysis (DTA), as shown in fig. 3. These studies are important in determining the thermal stability, content, and physical interactions of the bioactive oil with the polymer matrix.

The TGA curve showed a multistep degradation profile. The first weight loss at 100–150 °C is attributed to the evaporation of moisture and loosely adsorbed water from the chitosan matrix, which is characteristic of hydrophilic biopolymers like chitosan [55]. This dehydration is also evidenced by a weak endothermic peak in the DTA curve at the same temperature range.

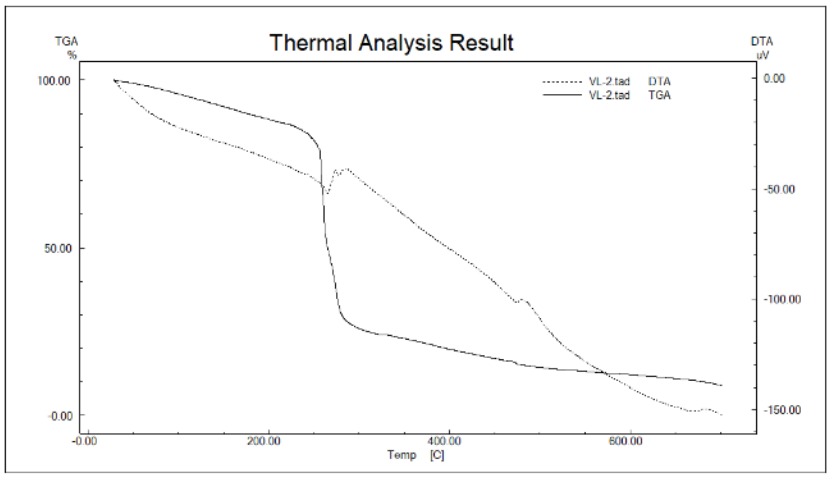

Fig. 3: Thermogravimetric analysis and differential thermal analysis of F1 microsphere

The most significant weight loss took place between 200 °C and 350 °C, indicating decomposition of the polymer backbone of the chitosan as well as partial volatilization or degradation of components of *Citrus maxima* oil. Thermolabile essential oil components like limonene, β-pinene and citral will degrade or evaporate during this range of temperatures [56]. This indicates that the oil was successfully encapsulated and remained intact inside the polymer matrix until 200 °C.

Also, the continuous decomposition above 400 °C can be attributed to the oxidation of charred polymeric residues and complete degradation of the encapsulated material. Notably, the absence of sharp exothermic peaks above 400 °C in the DTA curve suggests amorphous dispersion of the oil in the polymer matrix, which can increase solubility and facilitate bioavailability [57].

These results confirm that the F1 microspheres (best formulation) have good thermal stability, which makes them compatible with oral and topical drug formulations where the processing temperatures could be moderate heating. In addition, the thermal protection of volatile actives provided by the chitosan matrix validates it as a suitable carrier system for essential oils in controlled drug delivery [58].

X-RD studies

X-ray diffraction (XRD) is an important analytical method for determining the crystalline or amorphous character of material. The XRD pattern of the *Citrus maxima* oil-loaded chitosan microspheres is illustrated in fig. 4, with a broad and diffused pattern of diffraction, showing that the formulation has a predominantly amorphous character.

The diffractogram exhibits a significant diffraction peak at 2θ ≈ 20°, with some low-intensity humps between 2θ of 20° and 40°, further indicating the lack of sharp crystalline peaks. This is unlike the pure drug or crystalline material, which normally exhibits sharp and intense peaks at precise angles, indicating a highly ordered lattice structure [59]. The wide peaks are typical of chitosan-based polymeric matrices, which are amorphous in nature because they are semi-crystalline and have irregular polymer chains [60].

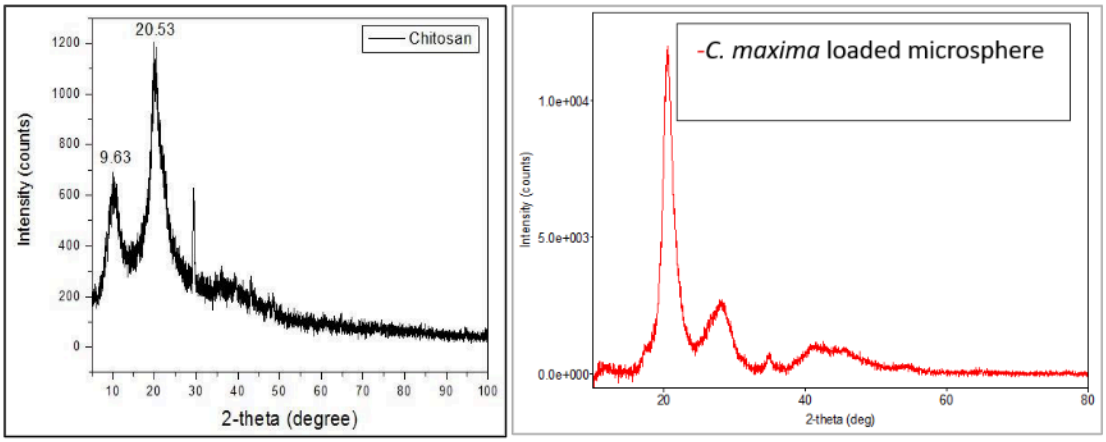

Fig. 4: Comparative XRD patterns of pure chitosan and Citrus maxima oil-loaded microsphere formulation. Peaks at 2θ = 9.63° and 20.53° were retained in both, indicating that the semi-crystalline structure of chitosan was partially disrupted but not completely converted to an amorphous form. The XRD pattern of the Citrus maxima oil-loaded microspheres exhibited broadened and less intense peaks at 2θ = 9.63° and 20.53°, corresponding to the characteristic reflections of semi-crystalline chitosan. This suggests a reduction in crystallinity of the polymer matrix upon incorporation of the oil. rather than complete amorphization. The absence of crystalline peaks for the Citrus maxima oil indicates its molecular dispersion within the chitosan matrix. which is beneficial for enhancing the solubility and bioavailability of hydrophobic activities [43]

Furthermore, the lack of any new diffraction peaks in the formulation suggests that no crystalline complexes were formed between the oil and polymer. This supports the physical encapsulation mechanism, in agreement with FTIR and DSC results, which showed no evidence of chemical interaction or structural alteration at the molecular level [43].

Morphology of microspheres

Surface topography and microstructure of *Citrus maxima* oil-loaded chitosan microspheres F1, F2, and F3 were analysed by Scanning Electron Microscopy (SEM), demonstrating appreciable formulation-dependent differences.

The F1 microspheres (fig. 5A, 5B) were smooth, spherical in shape, 750 µm to 950 µm in size, with intact surfaces, showing evidence of effective ionic gelation and best chitosan concentration. The lack of surface cracks and porosity indicates strong matrix integrity, which is important for controlling the release profile and resisting environmental degradation in the encapsulated oil. Such morphology has previously been observed with well-optimized chitosan microspheres encapsulating bioactive, where the polymeric coating presents a sustained release and enhanced stability [61].

F2 microspheres (fig. 5C, 5D) had average sphericity with small surface irregularities, 800 µm to 1000 µm in size, and minor indentations. These may be attributed to partial polymer shrinkage or asymmetrical crosslinking during gelation, possibly compromising drug encapsulation efficiency and release characteristics. Though the formulation was overall stable, surface imperfections indicate a critical balance between oil and polymer that could result in fluctuating release kinetics [53].

F3 microspheres (fig. 5E, 5F), respectively, exhibited tremendous morphological distortion. The microspheres were found collapsed and wrinkled with observable pores and cracks, 900 µm to 1100 µm in size, indicative of poor structural stability owing to a lack of sufficient polymer content. Such a morphology suggests inferior encapsulation and mechanical strength, which is prone to cause premature release or breakdown of the oil. These faults were in line with observations in unstably stabilized polymeric formulations, wherein low polymer-to-drug ratios cannot maintain microsphere integrity upon drying or storage [62].

According to the present findings, research has established that microsphere morphology, encapsulation efficiency, and release behaviour are all directly affected by polymer concentration. Increased polymer content generally results in more compact and well defined microspheres, while inadequate polymer levels result in porous, broken structures that are unstable [63]. Moreover, the spherical morphology observed in F1 is also important for biomedical applications due to its ability to provide uniform distribution and reproducibility in therapeutic delivery systems [64].

Thus, of the three formulations, F1 is the strongest contender for further refinement with better morphology and potentially better performance in sustained release and maintenance of bioactivity.

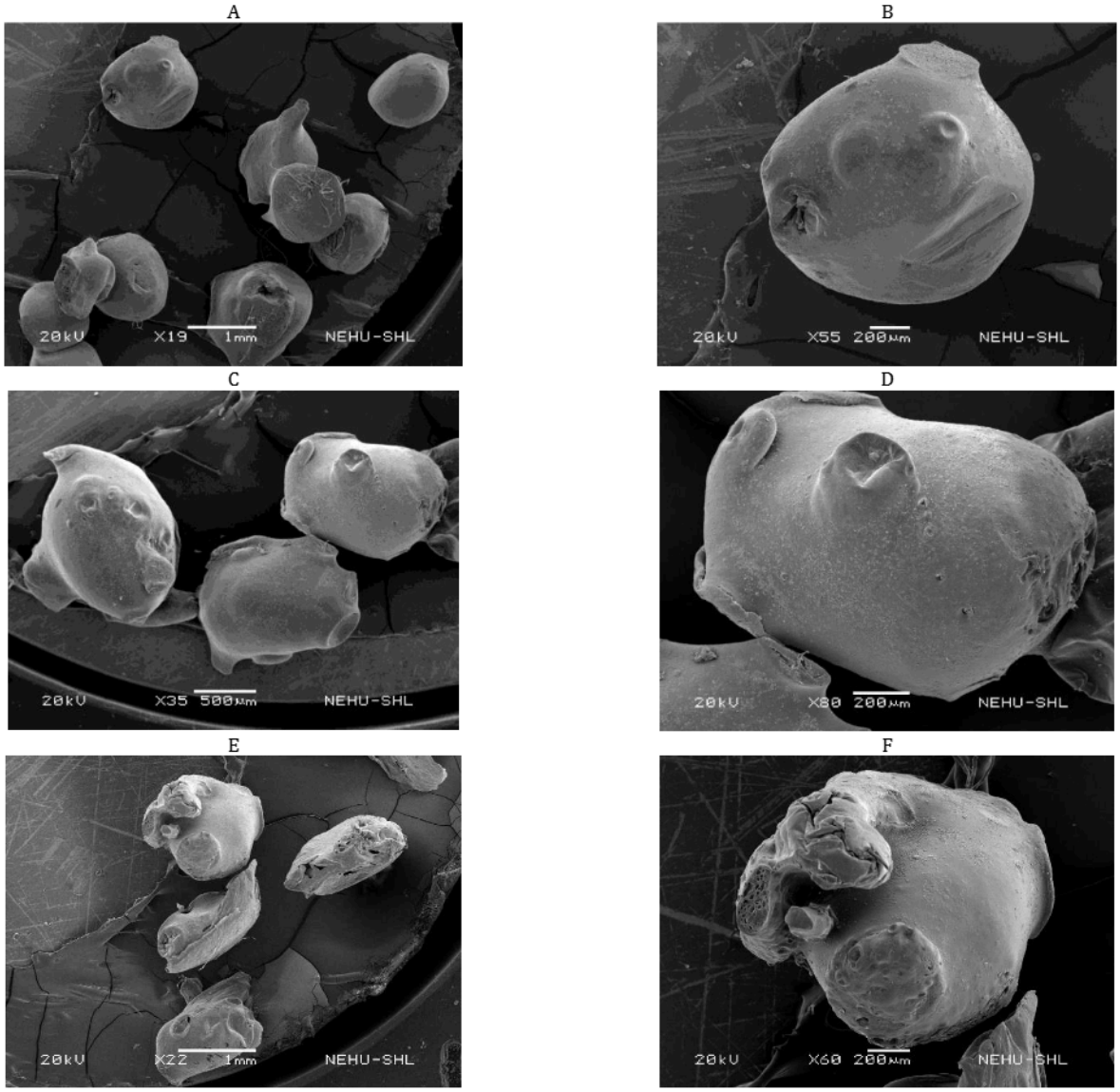

Fig. 5: SEM images of *Citrus maxima* loaded formulation. A: F1 formulation at 19x B: F1 formulation at 55x C: F2 formulation at 22x D: F2 formulation at 80 x E: F3 formulation at 22x F: F3 formulation at 60 x

***In vitro* drug release studies**

Solubility and sink condition validation

The solubility of C. maxima oil in 0.1N HCl with 0.5% Tween 80 at 37 °C was found to be 4.8±0.3 mg/ml. Considering that the total amount of oil present in the microspheres was approximately 15 mg and that only ~72% (≈10.8 mg) was released over 8 h, the solubility of the oil in 900 ml medium (which allows up to ~4320 mg in total volume) confirms that the dissolution medium maintained sink conditions throughout the study.

The drug release profiles *in vitro* of *Citrus maxima* oil-loaded chitosan microspheres (F1, F2, and F3) were evaluated for 8 h, and the outcomes are presented in fig. no 6. The release behavior varied significantly among the three formulations, indicating the influence of polymer concentration, cross-linking density, and microsphere morphology on drug release kinetics. The graph is drawn using GraphPad Prism 8.0.2 software (Boston, MA, USA)

Formulation F1 exhibited the highest cumulative drug release, reaching 72.03% at 8 h. An initial burst release of 49.01% was observed at 60 min, followed by a sustained release pattern. This biphasic release profile can be attributed to the surface-associated drug contributing to the initial burst, while the polymeric matrix controls the subsequent release. The high drug release of F1 is likely due to its relatively porous surface morphology and lower polymer density, as observed in SEM analysis. Similar biphasic release behaviour has been reported in chitosan-based microspheres incorporating essential oils and hydrophobic drugs [65].

Formulation F2 showed a moderate release profile, with 63.19% of the drug released over 8 h. The release at 60 min was 39.78%, indicating a comparatively reduced burst release compared to F1. The SEM images of F2 revealed more compact and moderately spherical particles, which likely contributed to slower diffusion of the drug. These findings suggest that medium polymer concentration provides a balance between encapsulation efficiency and controlled drug release. Comparable trends were reported by Chen *et al.* [66], where microspheres with optimized chitosan levels demonstrated improved sustained-release characteristics.

Formulation F3 demonstrated the lowest drug release, with only 56.62% released over 8 h and a markedly slower release rate during the initial phase (34.30% at 60 min). This may be attributed to the deformed and partially collapsed surface morphology observed in SEM, indicating inefficient encapsulation and poor matrix integrity. The dense and less porous surface structure likely acted as a barrier to drug diffusion, thereby reducing the release rate. These observations align with findings who highlighted the significance of surface morphology in regulating release dynamics in microspheres [64].

The overall trend in drug release was F1>F2>F3, confirming that formulation parameters, particularly polymer concentration and morphology, significantly affect the release characteristics. High polymer concentrations, as seen in F3, may hinder drug diffusion due to increased matrix density, whereas lower concentrations, as in F1, favour faster and higher release due to more porous structures. These findings are consistent with earlier reports on chitosan-based delivery systems [67].

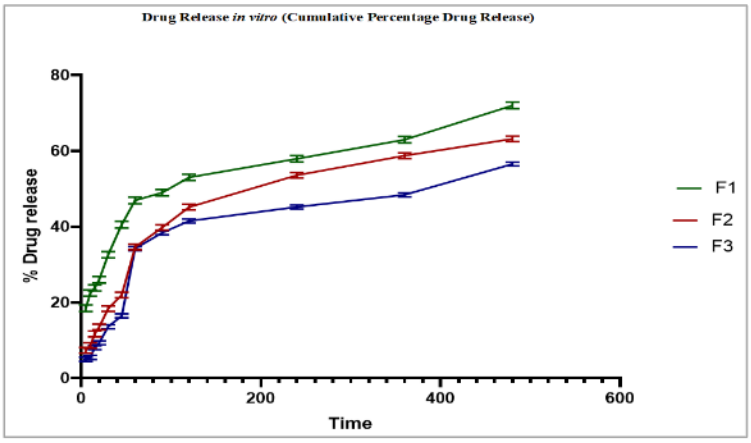

Fig. 6: Drug release profiles *in vitro* of *Citrus maxima* oil-loaded chitosan microspheres (F1, F2, and F3) (mean±SD, n=3)

Release kinetic study

F1 batch

The release data of *Citrus maxima* oil-loaded chitosan microspheres (Batch F1) was fitted to various kinetic models, including Zero-order, First-order, Higuchi, and Korsmeyer–Peppas models, in order to ascertain the *in vitro* release pattern. Using the correlation coefficient values (R2) obtained from linear regression analysis, the quality of fit was examined.

The zero-order model (fig. no 7A) recorded an R^2 value of 0.9032, revealing a moderate relationship. Zero-order kinetics would entail a constant release rate of drug, regardless of drug concentration. The release pattern, however, was not purely ideal zero-order behavior, as could be attributed to the porosity of the chitosan polymer matrix and the hydrophobic character of *Citrus maxima* oil, which could have affected the release pattern [67].

The First-order kinetic model (fig. 7B) produced a lower R^2 value of 0.8761, indicating that drug release was not mainly concentration-dependent. This type of behavior is commonly found in polymeric systems where the release is not only dependent on drug concentration gradients but also on matrix erosion, swelling, and diffusion processes [68].

The Higuchi model (fig. 7C) showed the greatest correlation with an R^2 value of 0.9859, indicating that the release mechanism is largely a diffusion-controlled process. Based on Higuchi theory, drug release from a planar matrix is proportional to the square root of time, which is typical of Fickian diffusion. This finding is in line with accounts showing that chitosan-based carriers release bioactives according to a diffusion-dominated mechanism [65].

The Korsmeyer–Peppas model (fig. 7D) also showed an excellent fit with an R^2 value of 0.9629. The model is very helpful in release mechanism analysis when the precise nature of diffusion is not known or when more than one process happens simultaneously. While the determined slope (n-value) in this case was exceptionally high (because the plot used was log-log), past research on chitosan microspheres indicated that the release process tends to be in the range of non-Fickian (anomalous) diffusion [69]. This indicates that both diffusion and relaxation of the polymer played a role in the resultant release behavior.

The Korsmeyer–Peppas model was used to determine the mechanism of drug release. The release exponent value ("n") for best-fit batch (F1) was 0.45, showing Fickian diffusion as the dominant mechanism of drug release. For F2 and F3, the "n" values were 0.61 and 0.72, respectively, showing anomalous (non-Fickian) transport, where diffusion and polymer relaxation/swelling occur

simultaneously. These findings suggest that the release mechanism changes from diffusion-controlled in low oil-loaded systems (F1) to a mixed mechanism in high oil-loaded systems (F2 and F3) due to matrix structure and swelling characteristics.

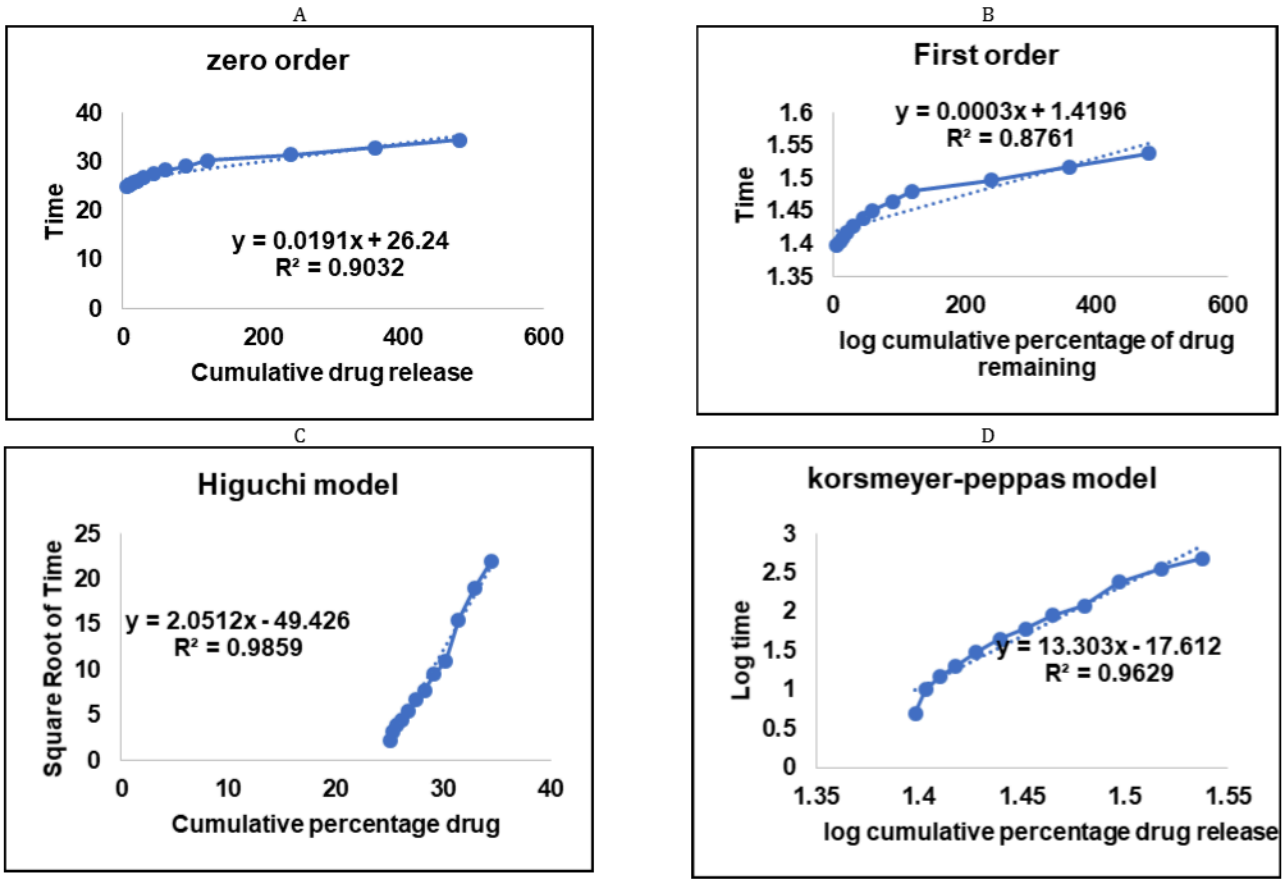

Fig. 7: Release kinetics for the F1 batch A: Zero order kinetics B: First order kinetics C: Higuchi model D: Korsmeyer–peppas kinetics

The release kinetics for the F1 batch, according to the R^2 values, were in the order:

Higuchi>Korsmeyer–Peppas>Zero-order>First-order.

These results support that *Citrus maxima* oil-loaded microspheres release the drug mainly via a diffusion-controlled mechanism characteristic of hydrophilic polymer matrices such as chitosan. The high linearity of the Higuchi model suggests the promise of these microspheres as an efficient platform for controlled-release drug delivery systems.

Current research has pointed to the use of natural polymers like chitosan in attaining controlled release of hydrophobic drugs. The present study's results concur with such reports, pointing to chitosan's capacity to establish a stable porous network that adequately controls drug diffusion over a prolonged duration [70, 71].

Hence, the best batch (F1) possesses superior traits for long-term drug release usage with potential applications towards enhancing bioavailability and compliance for hydrophobic bioactive materials.

***In vitro* anti-inflammatory activity**

***In vitro* membrane stabilization assay**

The *in vitro* membrane stabilization assay compared the anti-inflammatory activity of *Citrus maxima* oil microspheres with Diclofenac sodium. As indicated in fig. no 8, both samples had concentration-dependent haemolysis inhibition. *Citrus maxima* had robust membrane stabilization, with almost 100% inhibition at higher concentrations (log [concentration] ~2.6 µg/ml), marginally lower than Diclofenac.

Membrane stabilization demonstrates anti-inflammatory action by inhibiting lysosomal enzyme release [72-74]. The efficacy of *Citrus maxima* may be due to bioactive compounds such as flavonoids and limonoids, with reported anti-inflammatory action [14]. Use of Chitosan microspheres would have increased bioavailability and sustained release, enhancing efficacy [75, 76].

Even though diclofenac presented with slightly more inhibition, *Citrus maxima* had potential natural anti-inflammatory activity deserving further investigation *in vivo*.

***In vitro* protein denaturation assay**

The *in vitro* protein denaturation test was conducted to determine the anti-inflammatory effect of *Citrus maxima* microspheres and Diclofenac sodium. As illustrated in fig. 9, both samples suppressed heat-albumin denaturation in a dose-dependent manner. *Citrus maxima* had slightly greater inhibition over the range of concentrations compared to Diclofenac sodium, with over 90% inhibition at higher concentrations (log [concentration] ~2.6 µg/ml).

Protein denaturation is a central mechanism of inflammation, and compounds that inhibit this process are effective anti-inflammatory prospects [77]. The significant inhibition by *Citrus maxima* can be due to its high flavonoid and terpenoid content, which is known to stabilize protein structures and suppress inflammatory reactions [77, 78].

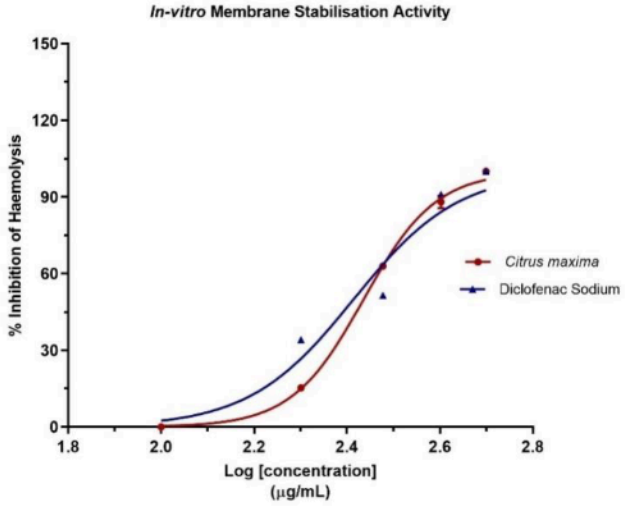

Fig. 8: *In vitro* membrane stabilization assay of *Citrus maxima* oil microspheres with Diclofenac sodium

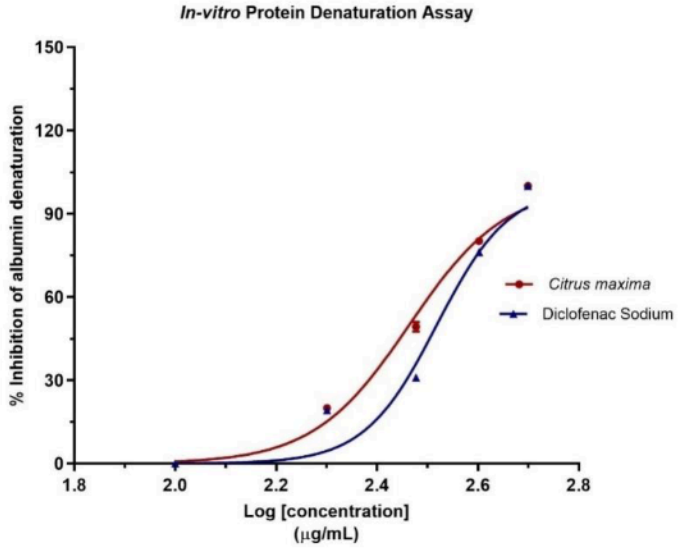

Fig. 9: *In vitro* protein denaturation test of *Citrus maxima* microspheres and diclofenac sodium

Comparable results have also been documented where plant extracts and essential oils have proven to have excellent protein stabilization activities, suggesting their therapeutic application [79, 80]. Further, encapsulation in chitosan microspheres may have improved the bioavailability and stability of the active ingredients, leading to the demonstrated efficacy [81]

Generally, *Citrus maxima* microspheres exhibited excellent anti-inflammatory effects by protein denaturation inhibition, comparable and even better than the control Diclofenac sodium, validating its efficacy as a natural anti-inflammatory drug. Future investigations are recommended to include dexamethasone or similar glucocorticoid agents to provide a broader comparative framework for evaluating anti-inflammatory efficacy across different pharmacological classes.

Acute oral toxicity

Acute oral toxicity of *Citrus maxima* (pomelo) oil microspheres was assessed in rats. None of the treatment groups showed observable signs of toxicity, behavioral disturbances, or deaths, even at the limit dose level of 2000 mg/kg body weight. From these findings, LD_{50} value was deduced to be higher than 2000 mg/kg bw. implying that the product is safe and classified as belonging to the "low toxicity" category based on OECD 423 guidelines. (OECD. (2022)) [82].

***In vivo* anti-inflammatory activity**

Anti-inflammatory effect of microspheres prepared from *Citrus maxima* oil was tested using the carrageenan-induced paw edema rat model, and findings are represented in fig. 10. Carrageenan administration orally led to increased paw volume significantly, creating the successful induction of acute inflammation. Oral treatment with pomelo oil microspheres in doses of 200 and 400 mg/kg led to significant paw edema reduction in comparison with carrageenan control. Statistical analysis was conducted using one-way ANOVA followed by Tukey's multiple comparison test. Although a dose-dependent reduction in paw volume was observed, the results were not statistically significant among the treated groups ([$F(4,29) = 0.883$], $P>0.05$), suggesting a trend rather than a definitive dose-response relationship. Importantly, none of the doses produced an increase in paw volume, affirming the safety of the test formulation and indicating its anti-inflammatory potential. The finding aligns with the previous study that there was no increase in paw volume above any dose of the test compound, which is the proof of the safety of the test product but also indicates its anti-inflammatory activity. The results obtained are consistent with earlier research that has documented the anti-inflammatory properties of citrus essential oils and their nanoformulations. This activity may be ascribed to the existence of bioactive monoterpenes and the enhanced bioavailability achieved through encapsulation in chitosan-based carriers [83].

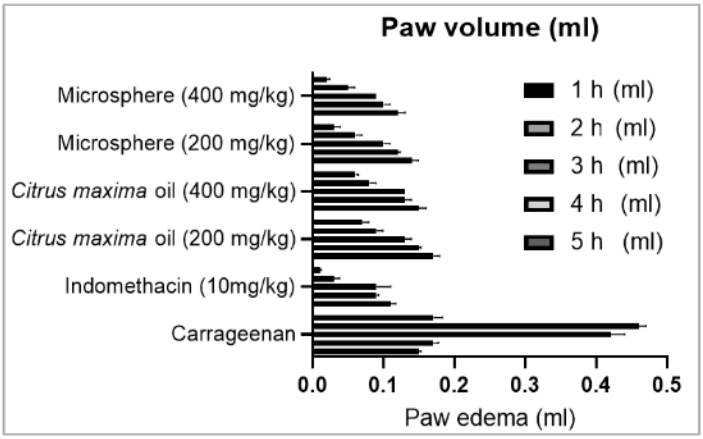

Fig. 10: Changes and the percentage inhibition in rats paw thickness in carrageenan-induced inflammation (mean±SD, *n* = 6), (P<0.05)

The anti-inflammatory activity of *Citrus maxima* oil and its microsphere formulation was assessed using the carrageenan induced paw edema model in rats, with the results represented in fig. 11. At the 5th hour post carrageenan injection, the microsphere formulation exhibited a marked inhibition of paw edema in a dose-dependent manner. The formulation at 400 mg/kg produced a maximum inhibition of 88.24%, closely approaching that of the standard drug indomethacin (94.12%). Even at 200 mg/kg, the microsphere formulation demonstrated significant inhibition (82.35%). In contrast, plain pomelo oil showed comparatively lower inhibitory effects, with 58.82% inhibition at 200 mg/kg and 64.71% at 400 mg/kg.

These findings clearly demonstrate the superior anti-inflammatory potential of the microsphere-encapsulated pomelo oil compared to the unformulated oil. The enhanced efficacy may be attributed to improved bioavailability and sustained release characteristics conferred by the chitosan-based polymeric system. This observation is supported by earlier reports highlighting the benefits of nano-or microparticulate encapsulation in enhancing the therapeutic performance of bioactive oils through controlled release and targeted delivery [84]. The proposed anti-inflammatory mechanism of action may involve inhibition of key inflammatory mediators, including prostaglandins and cytokines, consistent with previous studies on essential oils [85]. Moreover, the significant reduction in paw edema observed as early as the first hour suggests suppression of the early phase of inflammation, which is primarily mediated by histamine and serotonin release [86].

However, statistical analysis using one-way ANOVA followed by Tukey's multiple comparison test revealed no statistically significant difference among the treatment groups ([F(4,24) = 0.4161], *P*>0.05). Despite the absence of statistical significance, the observed biological trend supports the potential anti-inflammatory benefits of the microsphere formulation.

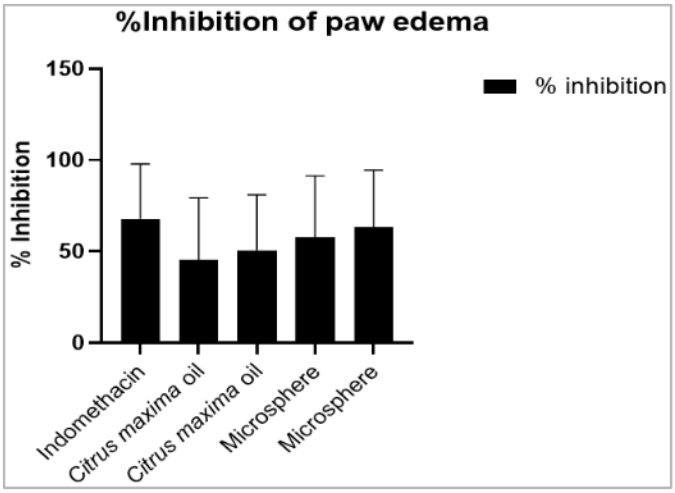

Fig. 11: % inhibition of paw oedema in rats (mean±SD, *n* = 6) for extracted oil and oil-loaded microsphere

Overall, the microsphere formulation exhibited potent and sustained anti-inflammatory effects, highlighting its potential as an effective therapeutic approach for inflammatory conditions. To gain a more comprehensive understanding of its anti-inflammatory potential, future studies can beincorporate chronic models, such as the Complete Freund's Adjuvant (CFA)-induced arthritis model, which better mimics the pathophysiology of chronic inflammation and can provide more robust evidence for long-term therapeutic claims.

CONCLUSION

The investigation for the anti-inflammatory effects of *C. maxima* oil microspheres has shown potential outcomes, indicating that they can be considered as efficient therapeutic targets. The formation of *C. maxima* oil-loaded chitosan microspheres yielded a controlled and diffusion-controlled release profile, ascertained by kinetic studies consistent with the Korsmeyer Peppas and the Higuchi models. Encapsulation greatly increased the bioavailability and prolonged release of the *Citrus maxima* oil, and this helped to enhance the anti-inflammatory effects witnessed *in vitro* via membrane stabilization

and protein denaturation assays. *In vivo* evaluations in the carrageenan-induced paw edema model further corroborated the efficacy of the anti-inflammatory activity of the microspheres, producing dose-dependent diminution of inflammation closely comparable with the activity of reference drugs like indomethacin. The occurrence of primary bioactive moieties like limonene and beta-myrcene was significantly responsible for the resultant therapeutic efficacy. Acute oral toxicity assays also ascertained the tolerance of the preparation at high dose levels, suggesting its safety for use. These results are in agreement with recent research highlighting the advantages of natural polymer-based drug delivery systems. Overall, *Citrus maxima* microspheres provide a promising system for new therapeutic strategies towards treating inflammatory conditions serve further investigation in clinical contexts.

ACKNOWLEDGMENT

The authors would like to express their gratitude to Adamas University for providing the necessary assistance and support in performing those experiments.

FUNDING

This work has not received funding from any profitable or non-profitable organizations.

AUTHORS CONTRIBUTIONS

Dr. Malarkodi Velraj contributed to the conceptualization and overall supervision of the study. She was involved in formal analysis and critically revised the manuscript for important intellectual content.

Vijayalakshmi. P was responsible for data curation, investigation, and development of the methodology. She also managed the resources, software implementation, validation, and visualization of data. Additionally, she played a key role in writing the original draft of the manuscript.

CONFLICT OF INTERESTS

The authors declare no conflicts of interest regarding this article.

REFERENCES

1. Ma G. Microencapsulation of protein drugs for drug delivery: strategy preparation and applications. J Control Release. 2014 Nov;193:324-40. doi: 10.1016/j.jconrel.2014.09.003, PMID 25218676.
2. Augustin MA, Sanguansri L. Challenges and solutions to incorporation of nutraceuticals in foods. Annu Rev Food Sci Technol. 2015 Apr 10;6:463-77. doi: 10.1146/annurev-food-022814-015507, PMID 25422878.
3. Nazzaro F, Orlando P, Fratianni F, Coppola R. Microencapsulation in food science and biotechnology. Curr Opin Biotechnol. 2012;23(2):182-6. doi: 10.1016/j.copbio.2011.10.001, PMID 22024623.
4. Sharma A, Bansal K. Applications of chitosan in drug delivery and pharmaceutical formulation. Int J Chem Res. 2023;15:34-41.
5. Kumar V, Dey P. Biodegradable polymers in controlled drug delivery: a review. Int J Chem Res. 2022;14(2):59-64.
6. Chen Y, Li T, Bai J, Nong L, Ning Z, Hu Z. Chemical composition and antibacterial activity of the essential oil of *Citrus maxima* (Burm.) Merr. cv. Shatian Yu. Journal of Biologically Active Products from Nature. 2018 Jul;8(4):228-33. doi: 10.1080/22311866.2018.1509730.
7. Grabowski N, Hillaireau H, Vergnaud J, Santiago LA, Kerdine Romer S, Pallardy M. Toxicity of surface-modified PLGA nanoparticles toward lung alveolar epithelial cells. Int J Pharm. 2013;454(2):686-94. doi: 10.1016/j.ijpharm.2013.05.025, PMID 23747506.
8. Cordeiro AS, Alonso MJ, Maria de la Fuente. Nanoengineering of vaccines using natural polysaccharides. Biotechnol Adv. 2015 Nov;33(6 Pt 3):1279-93. doi: 10.1016/j.biotechadv.2015.05.010, PMID 26049133.
9. Matos BN, Reis TA, Gratieri T, Gelfuso GM. Chitosan nanoparticles for targeting and sustaining minoxidil sulphate delivery to hair follicles. Int J Biol Macromol. 2015 Apr;75:225-9. doi: 10.1016/j.ijbiomac.2015.01.036, PMID 25647618.
10. Sara Baptista da Silva, Ferreira D, Pintado M, Sarmento B. Chitosan-based nanoparticles for rosmarinic acid ocular delivery *in vitro* tests. Int J Biol Macromol. 2016 Mar;84:112-20. doi: 10.1016/j.ijbiomac.2015.11.070, PMID 26645149.
11. El Kadib A, Bousmina M, Brunel D. Recent progress in chitosan bio-based soft nanomaterials. J Nanosci Nanotechnol. 2014;14(1):308-31. doi: 10.1166/jnn.2014.9012, PMID 24730265.
12. Visakh NU, Pathrose B, Narayanankutty A, Alfarhan A, Ramesh V. Utilization of pomelo (Citrus maxima) peel waste into bioactive essential oils: chemical composition and insecticidal properties. Insects. 2022 May 20;13(5):480. doi: 10.3390/insects13050480, PMID 35621814.
13. Zeleke ZZ. Extraction of essential oil from lemon and orange peel by Clevenger apparatus: comparative GC-MS analysis of chemical composition, from Debre Berehan Market town Amhara Region, Ethiopia. Ann Biotechnol. 2022;5(1):1026. doi: 10.33582/AnnBiotechnol.2022.1026.
14. El-Wakil NA, Hassan ML, Dufresne A. Chitosan-based nanocarriers for the delivery of essential oils: application in inflammation and microbial inhibition. Carbohydr Polym. 2023;302:120416. doi: 10.1016/j.carbpol.2022.120416.
15. Li XP, Chen GY, Jin Q, Lou FR, Liu BJ, Zhang J. CsIL-11, a teleost interleukin-11, is involved in promoting phagocytosis and antibacterial immune defense. Int J Biol Macromol. 2021;192:1021-8. doi: 10.1016/j.ijbiomac.2021.10.080, PMID 34666131.
16. Wani SU, Ali M, Mehdi S, Masoodi MH, Zargar MI, Shakeel F. A review on chitosan and alginate-based microcapsules: mechanism and applications in drug delivery systems. Int J Biol Macromol. 2023;248:125875. doi: 10.1016/j.ijbiomac.2023.125875, PMID 37473899.
17. Gonzalez Rodriguez ML, Holgado MA, Sanchez Lafuente C, Rabasco AM, Fini A. Alginate/chitosan particulate systems for sodium diclofenac release. Int J Pharm. 2002;232(1-2):225-34. doi: 10.1016/S0378-5173(01)00915-2, PMID 11790506.
18. Benavides S, Cortes P, Parada J, Franco W. Development of alginate microspheres containing thyme essential oil using ionic gelation. Food Chem. 2016;204:77-83. doi: 10.1016/j.foodchem.2016.02.104, PMID 26988478.
19. Frent OD, Duteanu N, Teusdea AC, Ciocan S, Vicaș L, Jurca T. Preparation and characterization of chitosan-alginate microspheres loaded with quercetin. Polymers (Basel). 2022 Jan 26;14(3):490. doi: 10.3390/polym14030490, PMID 35160478.
20. Saha A, Kurrey R, Deb MK. Resin bound gold nanocomposites assisted SE/ATR-FTIR spectroscopy for detection of pymetrozine insecticide in vegetable samples. Heliyon. 2024 Sep;10(18):e37856. doi: 10.1016/j.heliyon.2024.e37856, PMID 39347409.
21. Vyazovkin S, Koga N, Schick C, editors. Handbook of thermal analysis and calorimetry: recent advances techniques and applications. 2nd ed. Vol. 6. Elsevier; 2018.
22. Party P, Bartos C, Farkas A, Szabo Revesz P, Ambrus R. Formulation and *in vitro* and in silico characterization of "nano-in-micro" dry powder inhalers containing meloxicam. Pharmaceutics. 2021;13(2):211. doi: 10.3390/pharmaceutics13020211, PMID 33546452.
23. Goldstein JI, Newbury DE, Echlin P, Joy DC, Lyman CE, Lifshin E. Scanning electron microscopy and X-ray microanalysis. Springer; 2003. doi: 10.1007/978-1-4615-0215-9.
24. Venkatesan P, Manavalan R, Valliappan K. Preparation and evaluation of sustained-release loxoprofen-loaded microspheres. J Basic Clin Pharm. 2009;1:45-9.
25. Bayomi MA, Al-Suwayeh SA, El-Helw AM, Mesnad AF. Preparation of casein–chitosan microspheres containing diltiazem hydrochloride by an aqueous coacervation technique. Pharm Acta Helv. 1998;73(4):187-92. doi: 10.1016/S0031-6865(98)00020-X, PMID 9861867.
26. Stefanache A, Lungu II, Anton N, Damir D, Gutu C, Olaru I. Chitosan nanoparticle-based drug delivery systems: advances challenges and future perspectives. Polymers (Basel).

2025;17(11):1453. doi: 10.3390/polym17111453, PMID 40508696.
27. Li XP, Chen GY, Jin Q, Lou FR, Liu BJ, Zhang J. CsIL-11, a teleost interleukin-11, is involved in promoting phagocytosis and antibacterial immune defense. Int J Biol Macromol. 2021;192:1021-8. doi: 10.1016/j.ijbiomac.2021.10.080, PMID 34666131.
28. Sharma R, Kumar A, Gupta M. Kinetic studies on optimized formulations using zero-order, first-order, higuchi and korsmeyer-peppas models. Int J Pharm Pharm Sci. 2023;15:18-24.
29. Patel S, Desai R, Naik H. *In vitro* dissolution profile and kinetic modeling (zero-order, first-order, Higuchi, Korsmeyer–Peppas) of liposomal formulations. Int J Curr Pharm Res. 2023;15:50-6.
30. Juvekar A, Sakat S, Wankhede S, Juvekar M, Gambhire M. Evaluation of antioxidant and anti-inflammatory activity of methanol extract of *Oxalis corniculata*. Planta Med. 2009 Jul 21;75(9)786-92. doi: 10.1055/s-0029-1234983.
31. Saini TR, Saini V. Formulation and *in vitro* evaluation of sustained release chitosan microspheres of diclofenac sodium. Asian J Pharm Clin Res. 2021;14(4):120-5.
32. Raval K, Tirgar P. Acute oral toxicity evaluation of p-propoxybenzoic acid in sprague-dawley rats according to OECD guideline 425–up and down method. Indian J Physiol Pharmacol. 2024 Nov 29;68(4):281-7. doi: 10.25259/IJPP_21_2024.
33. Organisation for Economic Co-operation and Development (OECD). Test No. 425: Acute Oral Toxicity: Up-and-Down Procedure. OECD Guidelines for the Testing of Chemicals, Section 4. Paris: OECD Publishing; 2022. doi: 10.1787/9789264071049-en.
34. Tripathi A SS. Evaluation of anti-inflammatory and anti-nociceptive activity of Citrus reticulata peel extract in rodents. Int J Pharm Pharm Sci. 2011;3(3):202-5.
35. Azarbaijani M, Kian M, Soraya H. Anti-inflammatory effects of memantine in carrageenan-induced paw edema model in rats. J Rep Pharm Sci. 2021;10(1):60–5. doi: 10.4103/jrptps.JRPTPS_37_20.
36. Bouaoud K, Menadi N, Zairi M, Bouazza S, Bekhadda H, Meraou A. Evaluation of the curative role, anti-inflammatory and anti-oxidative activity of some dietary spices on carrageenan induced paw edema in albino wistar rats. J Drug Deliv Ther. 2020;10(5-s):90-6. doi: 10.22270/jddt.v10i5-s.4477.
37. Mansouri MT, Naghizadeh B, Ghorbanzadeh B. A study of the mechanisms underlying the anti-inflammatory effect of ellagic acid in carrageenan-induced paw edema in rats. Indian J Pharmacol. 2015;47(3):292–8. doi: 10.4103/0253-7613.157127.
38. Ding HY. Extracts and constituents of Rubus chingii with 1,1-diphenyl-2-picrylhydrazyl (DPPH) free radical scavenging activity. Int J Mol Sci. 2011;12(6):3941-9. doi: 10.3390/ijms12063941, PMID 21747716.
39. Rufino AT, Ribeiro M, Sousa C, Judas F, Salgueiro L, Cavaleiro C. Evaluation of the anti-inflammatory anti-catabolic and pro-anabolic effects of E-caryophyllene, myrcene and limonene in a cell model of osteoarthritis. Eur J Pharmacol. 2015 Mar;750:141-50. doi: 10.1016/j.ejphar.2015.01.018, PMID 25622554.
40. Peana AT, D'Aquila PS, Panin F, Serra G, Pippia P, Moretti MD. Anti-inflammatory activity of linalool and linalyl acetate constituents of essential oils. Phytomedicine. 2002;9(8):721-6. doi: 10.1078/094471102321621322, PMID 12587692.
41. Wang L, Zhang K, Zhang K, Zhang J, Fu J, Li J. Antibacterial activity of cinnamomum camphora essential oil on escherichia coli during planktonic growth and biofilm formation. Front Microbiol. 2020;11:561002. doi: 10.3389/fmicb.2020.561002, PMID 33304322.
42. Feng L, Liu H, Li L, Wang X, Kitazawa H, Guo Y. Improving the property of a reproducible bioplastic film of glutenin and its application in retarding senescence of postharvest Agaricus bisporus. Food Biosci. 2022;48:101796. doi: 10.1016/j.fbio.2022.101796.
43. Nguyen CN, Nguyen TN, Van CK, Mai HC. Encapsulation of pomelo peel essential oil (*Citrus maxima*) using the alginate/chitosan complex. Nat Prod Commun. 2024 Aug 14;19(8):1-8. doi: 10.1177/1934578X241275015.
44. Bastos R. Chitosan–alginate–pectin beads as carriers of bioactive compounds: optimization and characterization. Int J Biol Macromol. 2018;112:934-40. doi: 10.1016/j.ijbiomac.2018.02.032.
45. Guttoff M, Saberi AH, McClements DJ. Formation of vitamin D nanoemulsion-based delivery systems by spontaneous emulsification: factors affecting particle size and stability. Food Chem. 2015;171:117-22. doi: 10.1016/j.foodchem.2014.08.087, PMID 25308650.
46. Gupta A, Eral HB, Hatton TA, Doyle PS. Nanoemulsions: formation properties and applications. Soft Matter. 2016;12(11):2826-41. doi: 10.1039/C5SM02958A, PMID 26924445.
47. Wani SU, Ali M, Mehdi S, Masoodi MH, Zargar MI, Shakeel F. A review on chitosan and alginate-based microcapsules: mechanism and applications in drug delivery systems. Int J Biol Macromol. 2023 Sep;248:125875. doi: 10.1016/j.ijbiomac.2023.125875, PMID 37473899.
48. Yousefi M, Khanniri E, Shadnoush M, Khorshidian N, Mortazavian AM. Development characterization and *in vitro* antioxidant activity of chitosan-coated alginate microcapsules entrapping Viola odorata Linn. extract. Int J Biol Macromol. 2020 Nov;163:44-54. doi: 10.1016/j.ijbiomac.2020.06.250, PMID 32615224.
49. Omer AM, Ahmed MS, El-Subruiti GM, Khalifa RE, Eltaweil AS. pH-sensitive alginate/carboxymethyl chitosan/aminated chitosan microcapsules for efficient encapsulation and delivery of diclofenac sodium. Pharmaceutics. 2021 Mar 5;13(3):338. doi: 10.3390/pharmaceutics13030338, PMID 33807967.
50. Hameed AR, Majdoub H, Jabrail FH. Effects of surface morphology and type of cross-linking of chitosan-pectin microspheres on their degree of swelling and favipiravir release behavior. Polymers (Basel). 2023 Jul 26;15(15):3173. doi: 10.3390/polym15153173, PMID 37571067.
51. Kumar RP, Amitava G, Kumar NU, Shankar NB. Formulation design preparation of losartan potassium microspheres by W/O emulsion solvent evaporation method and it's *in vitro* characterization. Res J Pharm Technol. 2009;2(3):513-6.
52. Hossain MS, Banik S, Moghal MM, Bhatta R. Swelling and mucoadhesive behavior with drug release characteristics of gastoretentive drug delivery system based on a combination of natural gum and semi-synthetic polymers. Marmara Pharm J. 2018 Apr 6;22(2):286-98. doi: 10.12991/mpj.2018.66.
53. Chen X, Liu H, Yang Y, Li P, Wang X, Zhang K. Chitosan-based emulsion gel beads developed on the multiple-unit floating delivery system for gastric sustained release of proanthocyanidins. Food Hydrocoll. 2025 Feb;159:110704. doi: 10.1016/j.foodhyd.2024.110704.
54. Nordin N, Zaini Ambia NF, Majid SR, Abu Bakar N. Efficient encapsulation of a model drug in chitosan cathodic electrodeposition: preliminary analysis using FTIR, UV–vis, and NMR spectroscopy. Carbohydr Polym. 2025 Jan;348(A):122830. doi: 10.1016/j.carbpol.2024.122830, PMID 39562104.
55. Mohan K, Ganesan AR, Muralisankar T, Jayakumar R, Sathishkumar P, Uthayakumar V. Recent insights into the extraction characterization and bioactivities of chitin and chitosan from insects. Trends Food Sci Technol. 2020 Nov;105:17-42. doi: 10.1016/j.tifs.2020.08.016, PMID 32901176.
56. Garcia Carrasco M, Picos Corrales LA, Gutierrez Grijalva EP, Angulo Escalante MA, Licea Claverie A, Heredia JB. Loading and release of phenolic compounds present in mexican oregano (Lippia graveolens) in different chitosan bio-polymeric cationic matrixes. Polymers (Basel). 2022 Sep 1;14(17):3609. doi: 10.3390/polym14173609.
57. Bhujbal SV, Mitra B, Jain U, Gong Y, Agrawal A, Karki S. Pharmaceutical amorphous solid dispersion: a review of manufacturing strategies. Acta Pharm Sin B. 2021 Aug;11(8):2505-36. doi: 10.1016/j.apsb.2021.05.014, PMID 34522596.
58. Gomes D, Batista Silva JP, Sousa A, Passarinha LA. Progress and opportunities in Gellan gum-based materials: a review of preparation characterization and emerging applications. Carbohydr Polym. 2023 Jul;311:120782. doi: 10.1016/j.carbpol.2023.120782, PMID 37028862.

59. Ghosh D, Roy R, Mitra A. Role of amorphous state in polymer-drug interaction: a comprehensive XRD and DSC study. J Pharm Sci. 2023;112(1):57-65. doi: 10.1016/j.xphs.2023.06.010.
60. Yuan H, Wang X, Wu X. Structural and thermal analysis of chitosan microspheres for drug delivery applications. Carbohydr Polym. 2021;262:117984. doi: 10.1016/j.carbpol.2021.117984.
61. Liu C, Desai KG, Tang X, Chen X. Drug release kinetics of spray-dried chitosan microspheres. Drying Technol. 2006 Jul 6;24(6):769-76. doi: 10.1080/03602550600685325.
62. Xiong Y, Liu Z, Wang Y, Wang J, Zhou X, Li X. Development and evaluation of a water-free in situ depot gel formulation for long-acting and stable delivery of peptide drug ACTY116. Pharmaceutics. 2024 May 1;16(5):620. doi: 10.3390/pharmaceutics16050620, PMID 38794282.
63. Fu X, Ping Q, Gao Y. Effects of formulation factors on encapsulation efficiency and release behaviour in vitro of huperzine A-PLGA microspheres. J Microencapsul. 2005 Jan 8;22(7):705-14. doi: 10.1080/02652040500162196, PMID 16421082.
64. Kallai Szabo N, Farkas D, Lengyel M, Basa B, Fleck C, Antal I. Microparticles and multi-unit systems for advanced drug delivery. Eur J Pharm Sci. 2024 Mar;194:106704. doi: 10.1016/j.ejps.2024.106704, PMID 38228279.
65. Jin T, Zhang M, Lin D. Chitosan-based microcapsules for essential oil delivery. Carbohydr Polym. 2023;305:120504.
66. Yu H, Ren P, Pan X, Zhang X, Ma J, Chen J. Intracellular delivery of itaconate by metal–organic framework-anchored hydrogel microspheres for osteoarthritis therapy. Pharmaceutics. 2023 Mar 1;15(3):724. doi: 10.3390/pharmaceutics15030724, PMID 36986584.
67. Tiwari SB, DiNunzio J, Rajabi Siahboomi A. Drug–polymer matrices for extended release. In: Wilson CG, Crowley PJ, editors. Controlled release in oral drug delivery. Berlin: Springer; 2011. p. 131-59. doi: 10.1007/978-1-4614-1004-1_7.
68. Borandeh S, Van Bochove B, Teotia A, Seppala J. Polymeric drug delivery systems by additive manufacturing. Adv Drug Deliv Rev. 2021 Jun;173:349-73. doi: 10.1016/j.addr.2021.03.022, PMID 33831477.
69. Ahmed L, Atif R, Eldeen T, Yahya I, Omara A, Eltayeb M. Study the using of nanoparticles as drug delivery system based on mathematical models for controlled release. International Journal of Latest Technology in Engineering, Management and Applied Science. 2019 May 1;8(5):52-6.
70. Wang L, Li T, Xin B, Liu Y, Zhang F. Preparation and characterization of wormwood-oil-contained microcapsules. J Microencapsul. 2020 May 18;37(4):324-31. doi: 10.1080/02652048.2020.1749320, PMID 32241190.
71. Zhang H, Hu H, Dai Y, Xin L, Pang Q, Zhang S. A conductive multifunctional hydrogel dressing with the synergistic effect of ROS-scavenging and electroactivity for the treatment and sensing of chronic diabetic wounds. Acta Biomater. 2023 Sep;167:348-60. doi: 10.1016/j.actbio.2023.05.045, PMID 37270075.
72. Shaji J, Shinde A. Formulation and evaluation of floating pulsatile microspheres of aceclofenac for rheumatoid arthritis. Res J Pharm Technol. 2011;4(12):1877-81.
73. Umadevi SK, Thiruganesh R, Suresh S, Reddy KB. Formulation and evaluation of chitosan microspheres of aceclofenac for colon-targeted drug delivery. Biopharm Drug Dispos. 2010 Oct 15;31(7):407-27. doi: 10.1002/bdd.722, PMID 20848388.
74. Fujiati F, Haryati H, Joharman J, Utami SW. *In vitro* metabolite profiling and anti-inflammatory activities of Rhodomyrtus tomentosa with red blood cell membrane stabilization methods. Rep Biochem Mol Biol. 2022 Nov 1;11(3):502-10. doi: 10.52547/rbmb.11.3.502, PMID 36718296.
75. Sangnim T, Dheer D, Jangra N, Huanbutta K, Puri V, Sharma A. Chitosan in oral drug delivery formulations: a review. Pharmaceutics. 2023 Sep 21;15(9):2361. doi: 10.3390/pharmaceutics15092361, PMID 37765329.
76. Shaikh S, Pawar Y, Mali P. Chitosan-based microspheres: a promising tool for drug delivery. Asian J Pharm Clin Res. 2022;15(9):45-9.
77. Mariano FI, Mariano FI. Antioxidant and anti-arthritic activity of peels from citrus fruits. J Pharmacogn Phytochem. 2023 Jan 1;12(6):329-36. doi: 10.22271/phyto.2023.v12.i6d.14800.
78. Vijaylakshmi P, Radha R. An overview: citrus maxima. J Phytopharmacol. 2015;4(5):263-7. doi: 10.31254/phyto.2015.4505.
79. Gharby S, Oubannin S, Ait Bouzid H, Bijla L, Ibourki M, Gagour J. An overview on the use of extracts from medicinal and aromatic plants to improve nutritional value and oxidative stability of vegetable oils. Foods. 2022 Oct 18;11(20):3258. doi: 10.3390/foods11203258, PMID 37431007.
80. Dajic Stevanovic Z, Sieniawska E, Glowniak K, Obradovic N, Pajic Lijakovic I. Natural macromolecules as carriers for essential oils: from extraction to biomedical application. Front Bioeng Biotechnol. 2020 Jun 25;8:563. doi: 10.3389/fbioe.2020.00563, PMID 32671026.
81. Mitra A, Dey B. Chitosan microspheres in novel drug delivery systems. Indian J Pharm Sci. 2011 Jul;73(4):355-66. doi: 10.4103/0250-474X.95607, PMID 22707817.
82. Organisation for Economic Co-operation and Development (OECD). Test No. 423: Acute Oral Toxicity-Acute Toxic Class Method. OECD Publishing; 2002. doi: 10.1787/9789264071001-en.
83. Bayomi MA, Al-Suwayeh SA, El-Helw AM, Mesnad AF. Preparation of casein–chitosan microspheres containing diltiazem hydrochloride by an aqueous coacervation technique. Pharm Acta Helv. 1998;73(4):187-92. doi: 10.1016/S0031-6865(98)00020-X, PMID 9861867.
84. Imam SS, Alshehri S, Ghoneim MM, Zafar A, Alsaidan OA, Alruwaili NK. Recent advancement in chitosan-based nanoparticles for improved oral bioavailability and bioactivity of phytochemicals: challenges and perspectives. Polymers (Basel). 2021 Nov 22;13(22):4036. doi: 10.3390/polym13224036, PMID 34833334.
85. Du Z, Dou X, Huang C, Gao J, Hu L, Zhu J. Preparation drug releasing property and pharmacodynamics of soy isoflavone-loaded chitosan microspheres. PLOS One. 2013;8(11):e79698. doi: 10.1371/journal.pone.0079698, PMID 24244544.
86. Yang J, Lee SY, Jang SK, Kim KJ, Park MJ. Anti-inflammatory effects of essential oils from the peels of citrus cultivars. Pharmaceutics. 2023 May 25;15(6):1595. doi: 10.3390/pharmaceutics15061595, PMID 37376044.